

# The right posterior parietal cortex mediates spatial reorienting of attentional choice bias

Received: 20 September 2022

Accepted: 2 August 2024

Published online: 13 August 2024

 Check for updatesAnkita Sengupta <sup>1,6</sup>, Sanjna Banerjee<sup>1,3,6</sup>, Suhas Ganesh <sup>1,4</sup>,  
Shrey Grover <sup>1,5</sup> & Devarajan Sridharan <sup>1,2</sup> 

Attention facilitates behavior by enhancing perceptual sensitivity (sensory processing) and choice bias (decisional weighting) for attended information. Whether distinct neural substrates mediate these distinct components of attention remains unknown. We investigate the causal role of key nodes of the right posterior parietal cortex (rPPC) in the forebrain attention network in sensitivity versus bias control. Two groups of participants performed a cued attention task while we applied either inhibitory, repetitive transcranial magnetic stimulation ( $n = 28$ ) or 40 Hz transcranial alternating current stimulation ( $n = 26$ ) to the dorsal rPPC. We show that rPPC stimulation – with either modality – impairs task performance by selectively altering attentional modulation of bias but not sensitivity. Specifically, participants' bias toward the uncued, but not the cued, location reduced significantly following rPPC stimulation – an effect that was consistent across both neurostimulation cohorts. In sum, the dorsal rPPC causally mediates the reorienting of choice bias, one particular component of visual spatial attention.

Attention enables us to rapidly select and accurately process behaviorally relevant information from our sensory environment. In particular, visuospatial attention allows us to devote sensory processing resources toward locations that are likely to contain behaviorally relevant stimuli. Such selection operates regardless of whether attention is directed voluntarily (endogenously) to accomplish a goal or attracted reflexively (exogenously) toward a salient stimulus<sup>1</sup>. The behavioral advantages of attention typically manifest as higher accuracy and faster reaction times at the attended location<sup>2</sup>. These improvements are mediated by at least one of two distinct psychophysical mechanisms: i) perceptual sensitivity enhancement, i.e., enhanced sensory processing of the attended stimulus, and ii) choice bias enhancement, i.e., a bias afforded to the attended stimulus during decisions<sup>3,4</sup>. It is unclear if these attention components are mediated by distinct, common, or overlapping neural substrates. Several recent studies that investigated this question have produced diverse, and sometimes contradictory, conclusions<sup>4–6</sup>.

Here, we investigate the causal role of the posterior parietal cortex (PPC) – a key node in the forebrain attention network<sup>1,7</sup> – in mediating sensitivity and bias. The PPC's involvement in visuospatial attention has been extensively studied, from early behavioral studies of spatial neglect in patients with parietal lesions<sup>8</sup> to more recent studies employing electrophysiology, neuroimaging, or neurostimulation<sup>9,10</sup>. The PPC represents both exogenous stimulus properties, such as salience and novelty, as well as endogenous features, including context and goal relevance, albeit in a spatially selective manner<sup>11,12</sup>. In particular, several studies have documented a specific advantage for the right hemispheric PPC (rPPC) in visuospatial attention<sup>13,14</sup>. Both dorsal and ventral regions of the rPPC have been shown to be involved in the control of visuospatial attention<sup>15</sup>.

Within the rPPC, different subdivisions have been hypothesized to play distinct roles in spatial attention<sup>15,16</sup>. In particular, a number of recent studies have proposed a specific role for dorsal rPPC nodes in the voluntary “reorienting” of attention<sup>17,18</sup>. Reorienting of spatial

<sup>1</sup>Centre for Neuroscience, Indian Institute of Science, Bangalore 560012, India. <sup>2</sup>Department of Computer Science and Automation, Indian Institute of Science, Bangalore 560012, India. <sup>3</sup>Present address: Foundation of Art and Health India, Bangalore 560066, India. <sup>4</sup>Present address: Verily Life Sciences, San Francisco, CA 94080, USA. <sup>5</sup>Present address: Department of Psychological and Brain Sciences, Boston University, Boston, MA 02215, USA. <sup>6</sup>These authors contributed equally: Ankita Sengupta, Sanjna Banerjee. ✉ e-mail: [sridhar@iisc.ac.in](mailto:sridhar@iisc.ac.in)

attention occurs in cued visuospatial attention tasks, or endogenous “Posner” cueing tasks, of the type shown in Fig. 1a. In such tasks, participants’ attention is directed to one of two (or more) locations with a spatial, probabilistic cue<sup>19</sup>. On each trial, the event of interest – in this case, a grating orientation change – has a significantly higher probability of occurrence at the cued location. Participants must detect and localize the orientation change, indicating both whether and where it occurred with one of 3 responses: change at the cued location, change at the uncued location, or no change. On each trial, rational observers would direct their attention to the cued location – the most likely location of change<sup>5</sup>. Nonetheless, on a small, but significant proportion of trials, when the change occurs at the uncued location, they must also reorient their attention away from the cued location.

Dorsal rPPC nodes, including the superior parietal lobule (SPL) and the intraparietal sulcus (IPS) have been implicated in such voluntary reorienting of attention<sup>7,15,17,18</sup>. In particular, the SPL is hypothesized to be involved in the spatial reorienting (shifts) of attention while the IPS is hypothesized to be involved in the attentional weighting of competing stimuli<sup>20</sup>. Moreover, IPS lesions resulted in slower reaction times for contralateral versus ipsilateral targets as well as slower

reaction times for invalidly cued targets compared to validly cued targets<sup>21</sup>, suggesting a specific role for this region in reorienting of attention toward invalidly cued targets. Despite this emerging literature, the precise role of the rPPC, and its functional sub-divisions, in mediating the distinct components of attention – sensitivity versus bias – remains unknown.

In this work, we employ two non-invasive brain stimulation protocols – transcranial magnetic stimulation (TMS) and transcranial alternating current stimulation (tACS) – to causally manipulate activity in the dorsal rPPC, to study its role in visuospatial attention. In particular, we address three key questions: i) does stimulating the rPPC produce a selective effect on attentional reorienting? ii) does the effect manifest as a change in perceptual sensitivity or choice bias? and iii) do the effects occur for stimuli in both hemifields? In one cohort of  $n = 28$  participants, we perturb the rPPC activity with an inhibitory TMS protocol – continuous theta burst stimulation (cTBS) – that has been shown to induce prolonged suppression of activity in the motor cortex<sup>22</sup>. In another cohort of  $n = 26$  participants, we apply online 40 Hz, sinusoidal high-density tACS over rPPC; a protocol that has been shown in many studies to yield functional inhibition of cortical

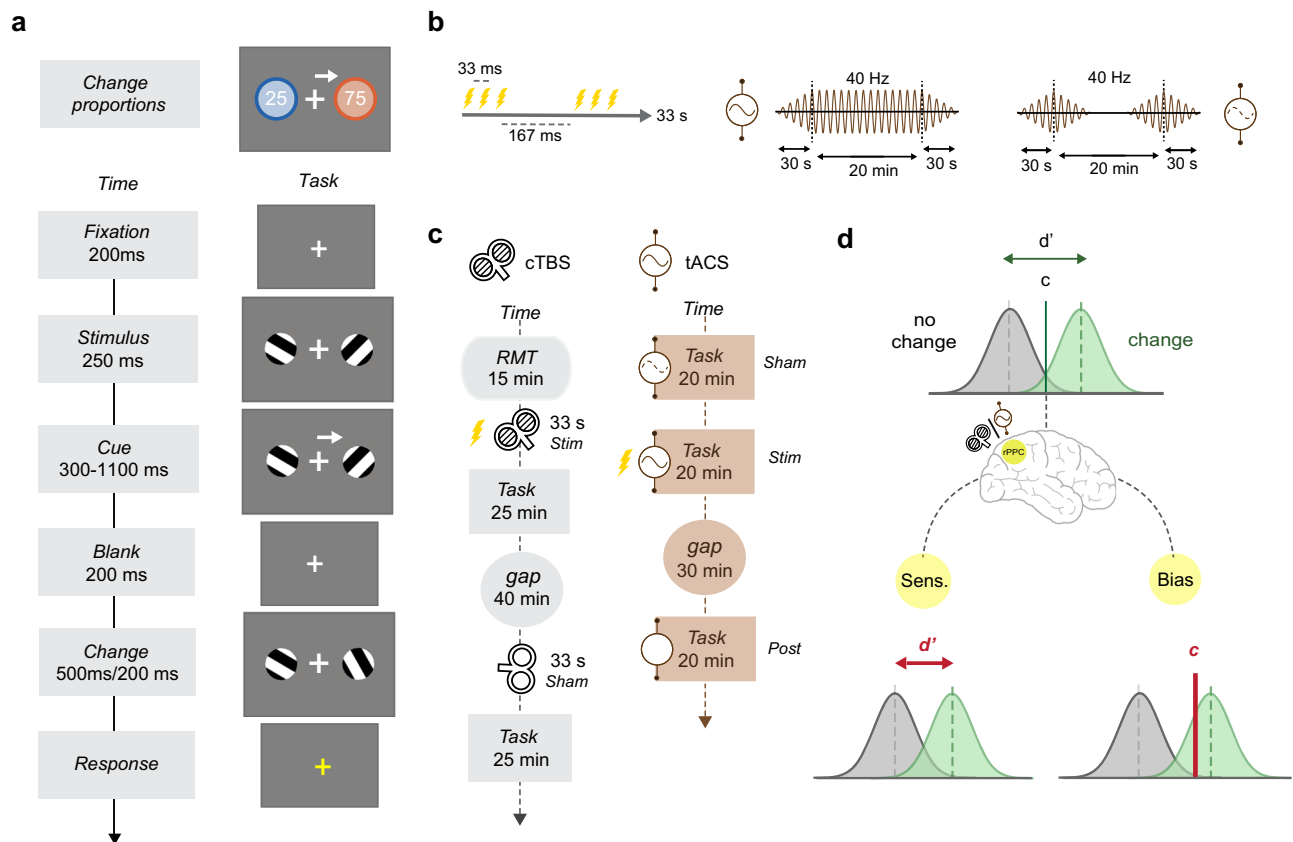


**Fig. 1 | Experimental protocol for testing the right PPC’s role in sensitivity versus bias control.** **a** Schematic of the cued attention task. Following a fixation epoch, two Gabor gratings appeared, one in each visual hemifield. This was followed by an attention cue (white arrow). The screen was then blanked briefly, and the gratings reappeared. Upon reappearance either one or none of the gratings had changed in orientation. The participant reported the location of “change” (left, right) or “no change” with one of three button presses. (Inset, top) A change occurred at the cued location in 75% (orange), and at the uncued location in 25% (blue), of “change” trials. **b** Stimulation protocols: (Left) cTBS involved 200 bursts of three pulses (yellow lightning symbol; inter-pulse interval: 33 ms, inter-burst interval: 167 ms). Sham cTBS was delivered with the same protocol, except that the coil was oriented orthogonally rather than tangentially. (Middle) tACS involved ramping up the current for 30 s to peak amplitude, which was maintained for 20 min, followed by a 30 s ramp down. (Right) Sham tACS involved ramping up (to peak) and down

the current for 30 s, at the beginning and end of the session. **c** (Left) cTBS experiment protocol: After resting motor threshold (RMT) determination, cTBS (real or sham) was delivered over rPPC, following which the participants performed five blocks of the cued attention task. After a washout period, cTBS (sham or real, respectively) was delivered again, and the participants performed another five task blocks. (Right) tACS experiment protocol: Participants performed a sham tACS session followed by a real tACS session, separated by a 5 min interval. A third (post) session, with no stimulation, followed after a 30 min interval. Participants performed five blocks of the attention task in each session. Session order was either counter-balanced (cTBS) or fixed (tACS) across participants. **d** (Top) Quantifying the effects of rPPC stimulation with signal detection theory. Green and gray Gaussians: signal (change) and noise (no change) decision variable distributions, respectively. (Bottom) rPPC stimulation may affect perceptual sensitivity ( $d'$ ) for detecting a change (left), or the criterion ( $c$ , bias) for reporting a change (right).

activity<sup>23,24</sup>. We measure participants' behavioral performance on an endogenous, cued attention task (Fig. 1a) and quantify sensitivity and bias at the cued and uncued locations, with a recent signal detection model, developed specifically for the analysis of attention tasks<sup>5,25,26</sup>. In both cases, we report a consistent decrease in bias at the uncued location following rPPC neurostimulation. The results indicate a causal role for the rPPC in reorienting one component of endogenous visual attention: spatial choice bias.

## Results

Two participant cohorts, comprising a total of  $n = 88$  participants (83 unique) participated in the neurostimulation experiments. Of these,  $n = 54$  participated in the main experiment, and the remaining participated in control experiments. Of the main experiment cohort,  $n = 28$  participated in the cTBS experiment and  $n = 26$  in the tACS experiment. In both cTBS and tACS experiments, participants performed an endogenously cued, multialternative, orientation change detection task (2-ADC task; Fig. 1a, b)<sup>25</sup>. Following fixation, two Gabor gratings were presented briefly, one in each hemifield. On each trial, a central attention cue (short arrow, Fig. 1a) directed participants to attend to one of the two gratings. After a variable interval, the screen was blanked, and the gratings reappeared. Upon reappearance, either one of the gratings had changed in orientation ("change" trials; 80%), or none had changed ("no change" trials; 20%). On change trials, cue validity was 75% (Fig. 1a, top inset). Participants indicated the event that they perceived – change at cued location, uncued location, or no change – by pressing one of three distinct buttons (for details, see Methods section on *Behavioral Task*). We investigated the effects of rPPC neurostimulation on both psychometric parameters (hit rates, false alarm rates, and reaction times) and psychophysical parameters (sensitivity and bias) (Methods; Supplementary Fig. S1a, b).

### Effects of rPPC cTBS on psychometric responses

Participants in the cTBS cohort ( $n = 28$ ) completed two sessions of the cued attention task (Fig. 1a) comprising 250 trials each, lasting 25 min, with a 40 min interval between sessions. Real cTBS (600 pulses delivered as 30 Hz bursts of 3 pulses with an inter-burst interval of 167 ms/6 Hz) was delivered immediately before one of the two task sessions (Methods section on *TMS experiments*; Fig. 1c, left). Sham cTBS was similarly delivered, except with the coil oriented orthogonal to the target site (see Discussion for choice of sham protocol). rPPC targets were identified with MR-guided neuro-navigation (AICHA atlas, BA 7<sup>27</sup>, Supplementary Fig. S2a); the cTBS protocol is more fully described in the Methods<sup>28</sup>. All behavioral results were compared between the stimulation and sham control sessions. The order of these sessions was counterbalanced across participants.

We evaluated the efficacy of the spatial cueing and neurostimulation protocols with two preliminary analyses. First, we tested whether participants indeed utilized the cue appropriately to direct their attention. Hit rates (proportion of correctly reported changes) were significantly higher ( $\Delta$ HR-sham (cued-uncued):  $z = 4.35$ ,  $p < 0.001$ , Wilcoxon signed rank test, Cohen's  $d = 1.87$ ,  $CI = [21.1, 38.7]\%$ ;  $\Delta$ HR-stim:  $z = 4.62$ ,  $p < 0.001$ , Cohen's  $d = 2.37$ ,  $CI = [27.9, 44.7]\%$ ; Fig. 2a, b) and reaction times were lower ( $\Delta$ RT-sham:  $z = -4.54$ ,  $p < 0.001$ , Cohen's  $d = 2.26$ ,  $CI = [-156, -93]$  ms;  $\Delta$ RT-stim:  $z = -4.18$ ,  $p < 0.001$ , Cohen's  $d = 1.79$ ,  $CI = [-155, -81]$  ms; Supplementary Fig. S3a) at the cued compared to the uncued location both during the sham and stimulation sessions, confirming that attention was indeed directed to the cued location. Second, we evaluated the persistence of the cTBS effects in a separate cohort of  $n = 7$  participants. For these participants, we delivered cTBS over the motor cortex, following which motor-evoked potentials (MEPs) were monitored every 10 min (Methods). The peak MEP amplitude dropped progressively and significantly until -50 min, when it was  $40.4 \pm 11.4\%$  (mean  $\pm$  std) of the pre-stimulation baseline ( $W = 21$ ,  $p = 0.031$ , Wilcoxon signed

rank test, Cohen's  $d = 5.23$ ,  $CI = [29.8, 50.9]\%$ ). However, at 60 min post cTBS stimulation, the MEP amplitude was numerically lower than, but not statistically significantly different from, baseline (mean  $\pm$  std =  $66.0 \pm 17.2\%$  of pre-stimulation baseline;  $W = 15$ ,  $p = 0.063$ , Wilcoxon signed rank test, Cohen's  $d = 1.98$ ,  $CI = [50.1, 81.9]\%$ ; Supplementary Fig. S2b, c). Nevertheless, there was a trend toward significance, potentially due to variable recovery among participants<sup>22,28,29</sup>. Due to a small cohort size and the absence of data beyond this time point (60 min), we concluded that the cTBS effects persist for at least 60 min. Therefore, in the main experiment, we ensured that all behavioral testing was conducted within this window following cTBS and that  $>60$  min had elapsed between the first cTBS stimulation and the behavioral testing in the sham cTBS session. In addition, we conducted a control analysis on the main cohort, and observed no statistically significant effect of the stimulation order ("sham first" versus "stim first") of cTBS on behavior at any location (SI Results section on *Additional control analyses for training and session order effects*).

cTBS over the right posterior parietal cortex (rPPC cTBS) produced a selective reduction in hit rates (proportion of changes detected correctly) at the uncued, but not the cued location. Following cTBS, hit rates did not change statistically significantly at the cued location (Fig. 2a, b) (cued: HR-sham =  $65.8 \pm 3.0\%$ , HR-stim =  $66.7 \pm 3.1\%$ ;  $\delta_{\text{cued}}$  (stim-sham):  $z = 1.48$ ,  $p = 0.139$ , Cohen's  $d = 0.23$ ,  $CI = [-1.3, 3.2]\%$ ), whereas hit rates decreased significantly at the uncued location (Fig. 2a, b) (uncued: HR-sham =  $35.9 \pm 2.9\%$ , HR-stim =  $30.4 \pm 3.3\%$ ;  $\delta_{\text{uncued}}$ :  $z = -2.37$ ,  $p = 0.017$ , Cohen's  $d = 0.70$ ,  $CI = [-9.9, -1.1]\%$ ). Consequently, attentional modulation of hit rates – quantified as the difference in hit rates between the cued and uncued locations ( $\Delta$ HR =  $HR_{\text{cued}} - HR_{\text{uncued}}$ ) – increased significantly following cTBS (Fig. 2e top left,  $\Delta$ HR-sham =  $29.8 \pm 4.3\%$ ,  $\Delta$ HR-stim =  $36.3 \pm 4.1\%$ ;  $\delta_{\Delta}$ :  $z = 2.48$ ,  $p = 0.013$ , Cohen's  $d = 0.70$ ,  $CI = [1.3, 11.5]\%$ ). On the other hand, false alarm rates (proportion of changes reported incorrectly on "no change" trials) were not statistically significantly different at any location (Fig. 2d) (cued: FAR-sham =  $29.8 \pm 3.1\%$ , FAR-stim =  $32.4 \pm 3.4\%$ ;  $\delta_{\text{cued}}$ :  $z = 1.09$ ,  $p = 0.275$ , Cohen's  $d = 0.37$ ,  $CI = [-1.3, 6.7]\%$ ; uncued: FAR-sham =  $14.6 \pm 1.6\%$ , FAR-stim =  $15.8 \pm 2.5\%$ ;  $\delta_{\text{uncued}}$ :  $z = 0.20$ ,  $p = 0.838$ , Cohen's  $d = 0.20$ ,  $CI = [-2.6, 5.1]\%$ ). As a consequence, the attentional modulation of false alarm rates was also not statistically significantly different (Fig. 2e bottom,  $\Delta$ FAR-sham =  $15.2 \pm 3.7\%$ ,  $\Delta$ FAR-stim =  $16.6 \pm 4.7\%$ ;  $\delta_{\Delta}$ :  $z = 0.28$ ,  $p = 0.775$ , Cohen's  $d = 0.13$ ,  $CI = [-4.7, 7.6]\%$ ). Following a Shapiro-Wilk test to identify non-normality (see Methods section on *Statistical tests*), we performed a two-way ANOVA to test for the effects of cueing (cued, uncued) and stimulation condition (sham, stim) on the parameters to confirm these results. We observed a significant main effect of cueing on hit rates ( $F_{1,27} = 68.42$ ,  $p < 0.001$ ) and also on false alarm rates ( $F_{1,27} = 16.24$ ,  $p = 0.004$ ), but no statistically significant main effect of stimulation condition on either metric ( $p > 0.05$ ). Nonetheless, there was a significant interaction between cueing and stimulation condition, but only on hit rates (HR:  $F_{1,27} = 6.74$ ,  $p = 0.015$ ; FAR:  $F_{1,27} = 0.23$ ,  $p = 0.636$ ). cTBS also produced systematic effects on the attentional modulation of mislocalization rates (MLR, Fig. 2c, e top right); these effects are described in the SI Results section on *Effects of neurostimulation on mislocalization responses*. Moreover, we observed no statistically significant effects of rPPC cTBS on reaction times or on its modulation by attention at any location (Supplementary Fig. S3a) (cued: RT-sham =  $527 \pm 17$  ms, RT-stim =  $509 \pm 20$  ms;  $\delta_{\text{cued}}$ :  $z = -1.18$ ,  $p = 0.236$ , Cohen's  $d = 0.44$ ,  $CI = [-42, 5]$  ms; uncued: RT-sham =  $655 \pm 13$  ms, RT-stim =  $626 \pm 23$  ms;  $\delta_{\text{uncued}}$ :  $z = -1.23$ ,  $p = 0.218$ , Cohen's  $d = 0.61$ ,  $CI = [-37, 6]$  ms;  $\Delta$ RT-sham =  $-124 \pm 15$  ms,  $\Delta$ RT-stim =  $-118 \pm 18$  ms;  $\delta_{\Delta}$ :  $z = 0.01$ ,  $p = 0.990$ , Cohen's  $d = 0.16$ ,  $CI = [-20, 21]$  ms).

In summary, rPPC cTBS produced a significant decrease in hit rates at the uncued location, suggesting a deficit in attentional reorienting for successfully detecting changes at the uncued location.

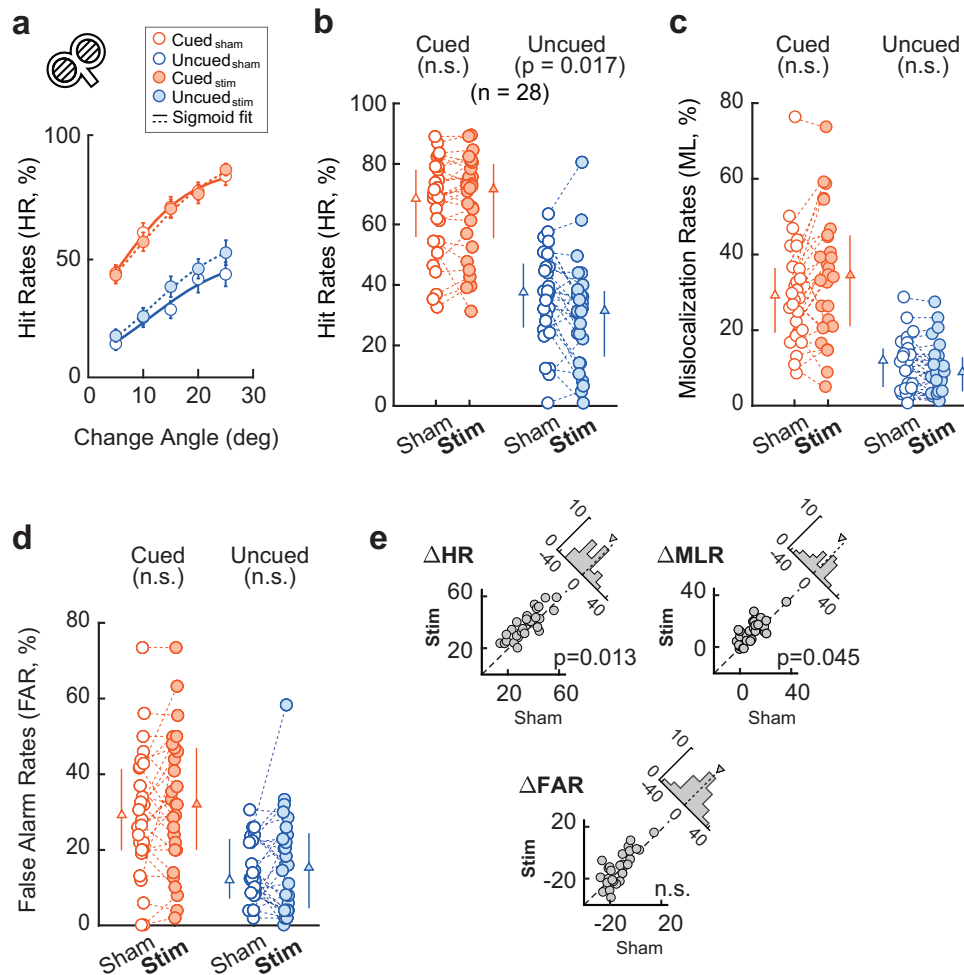


**Fig. 2 | Effects of rPPC cTBS on psychometrics.** **a** Psychometric functions of hit rates as a function of orientation change angle magnitude (average across  $n = 28$  participants) during the sham cTBS (Sham; open circles) session, indicative of baseline performance, and the real cTBS (Stim; filled circles) session. Orange and blue circles: hit rates at the cued and uncued locations, respectively. Curves: sigmoid fits. Error bars: s.e.m. **b** Hit rates (HR) for detecting changes at the cued (orange) and uncued locations (blue) in Sham (open circles) and Stim (filled circles) sessions, averaged over all change angles. Markers represent individual participants ( $n = 28$ ). Paired data from the same participant (across Sham and Stim sessions) are connected by dashed lines. Triangles denote median sham (open) and stim (filled) HR, lines denote the 25th and 75th percentile of each data set.  $p$ -values denote statistical significance levels assessed with a two-sided Wilcoxon signed rank test, followed by a Benjamini-Hochberg correction for multiple comparisons.

n.s.: not statistically significantly different at the  $p = 0.05$  level. **c** Same as in panel (b), but for mislocalization rates (MLR) at the cued (orange) and uncued (blue) locations. Other conventions are the same as in panel (b). **d** Same as in panel (b), but for false alarm rates (FAR) at the cued (orange) and uncued (blue) locations. Other conventions are the same as in panel (b). **e** (Top left) Attentional modulation of hit rates ( $\Delta HR = HR_{\text{cued}} - HR_{\text{uncued}}$ ) in the Sham (x axis) and Stim (y axis) sessions. Markers represent individual participants. Dashed line: line of equality. (Inset) Histogram of  $\Delta HR$  values across participants ( $n = 28$ ). Triangle denotes median  $\Delta HR$ . (Top right) Same as in the top left panel but for mislocalization rates ( $\Delta MLR = MLR_{\text{cued}} - MLR_{\text{uncued}}$ ). Other conventions are the same as in the top left panel. (Bottom) Same as in the top left panel but for false alarm rates ( $\Delta FAR = FAR_{\text{cued}} - FAR_{\text{uncued}}$ ). Other conventions are the same as in the top left panel.

Next, we tested whether this reorientation deficit could be attributed to sensitivity versus bias effects.

### Effects of rPPC cTBS on sensitivity and bias

We estimated sensitivity and bias, before and after neurostimulation, by fitting behavioral observations (Supplementary Fig. S1a) with a recent signal detection (m-ADC) model (Supplementary Fig. S1b; Methods section on *Estimating psychophysical parameters*); this model has been employed and validated in multiple recent studies investigating behavioral and neural mechanisms of attention<sup>5,6,25,30</sup>. Briefly, sensitivity at each location was quantified as the  $d'$ -index for distinguishing signal (“change”) from noise (“no change”). Bias was quantified with the choice criterion (c); the criterion is inversely related to choice bias such that a lower value of the criterion at a location indicates a higher bias for reporting change at that location (Methods section on *Estimating psychophysical*

*parameters*). Goodness-of-fit tests indicated that the m-ADC model fit the behavioral observations accurately (Supplementary Fig. S1c, randomization test).

rPPC cTBS produced no statistically significant effects on  $d'$  either at the cued location (cued:  $d'$ -sham =  $1.12 \pm 0.09$ ,  $d'$ -stim =  $1.06 \pm 0.10$ ;  $\delta_{\text{cued}}$ :  $z = -1.02$ ,  $p = 0.305$ , Cohen's  $d = 0.29$ ,  $CI = [-0.17, 0.06]$ ) or at the uncued location (uncued:  $d'$ -sham =  $0.73 \pm 0.07$ ,  $d'$ -stim =  $0.63 \pm 0.08$ ;  $\delta_{\text{uncued}}$ :  $z = -1.53$ ,  $p = 0.127$ , Cohen's  $d = 0.44$ ,  $CI = [-0.22, 0.02]$ ; Fig. 3a). Moreover, we observed no statistically significant effects on the attentional modulation of  $d'$  ( $\Delta d' = d'_{\text{cued}} - d'_{\text{uncued}}$ ) following cTBS ( $\Delta d'$ -sham =  $0.39 \pm 0.08$ ,  $\Delta d'$ -stim =  $0.43 \pm 0.08$ ;  $\delta_{\Delta}$ :  $z = 0.52$ ,  $p = 0.600$ , Cohen's  $d = 0.16$ ,  $CI = [-0.10, 0.18]$ ; Fig. 3c). We also analyzed the entire psychophysical function ( $d'$  as a function of change angle; Supplementary Fig. S4a): A two-way ANOVA revealed no statistically significant interaction between stimulus strength (change angle values, i.e.,  $\Delta\theta$ ) and stimulation condition on  $\Delta d'$  ( $F_{1,108} = 0.63$ ,  $p = 0.646$ ).



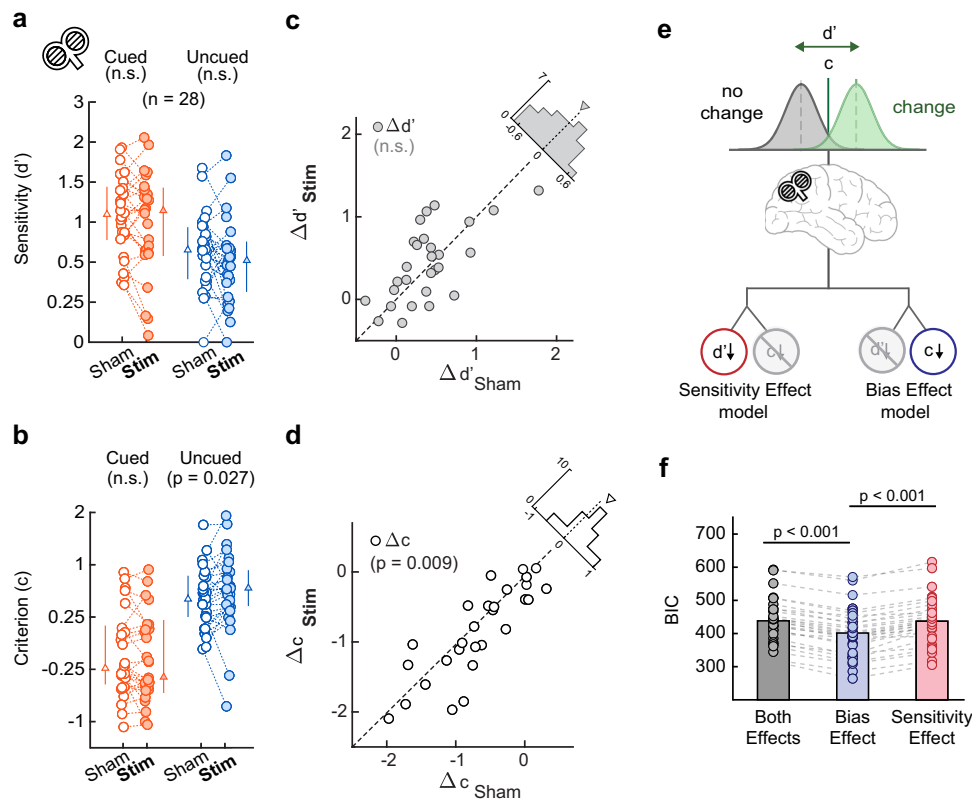


**Fig. 3 | Effects of rPPC cTBS on sensitivity and bias.** **a** Sensitivity ( $d'$ ) plotted in symmetrical logarithmic scale for detecting changes at the cued (orange) and uncued locations (blue) during the Sham cTBS (open circles) and Stim cTBS (filled circles) sessions ( $n = 28$  participants).  $p$ -values denote statistical significance levels assessed with a two-sided Wilcoxon signed rank test, followed by a Benjamini-Hochberg correction for multiple comparisons. n.s.: not statistically significantly different at the  $p = 0.05$  level. Other conventions are the same as in Fig. 2b. **b** Same as in panel (a), but for criterion (c). A lower value of the criterion at a location indicates a higher choice bias for reporting a change at that location. Other conventions are the same as in Fig. 2b. **c**. Attentional modulation of sensitivity ( $\Delta d' = d'_{\text{cued}} - d'_{\text{uncued}}$ ; grey circles) in the Sham (x axis) and Stim (y axis) sessions. (Top right inset) Histogram of  $\Delta d'$  values across participants ( $n = 28$ ). Other conventions

are the same as in Fig. 2e. **d**. Same as in panel (c), but for criterion ( $\Delta c = c_{\text{cued}} - c_{\text{uncued}}$ ; open circles). Other conventions are the same as in Fig. 2e. **e** Schematic of model comparison analysis for rPPC cTBS effects. Signal detection models in which rPPC stimulation produced only a sensitivity change (“sensitivity-effect” model, left) or only a criterion change (“bias-effect” model, right) were compared against the standard signal detection model (“both effects”). **f** Mean Bayesian Information Criterion (BIC) scores for the both-effects (grey), bias-effect (blue) and sensitivity-effect (red) models for the cTBS cohort. Markers represent individual participants ( $n = 28$ ). Dashed lines connect each participant’s BIC scores across models. Error bars: s.e.m.  $p$ -values denote statistical significance levels, assessed with a two-sided Wilcoxon signed rank test, followed by a Benjamini-Hochberg correction for multiple comparisons.

Therefore, sensitivity changes were unlikely to account for the strong effects of stimulation on hit rates.

On the other hand, rPPC cTBS produced systematic effects on criteria in a manner that mimicked the effects on hit rates. Although criteria at the cued location were not statistically significantly affected following cTBS (cued:  $c_{\text{sham}} = -0.14 \pm 0.09$ ,  $c_{\text{stim}} = -0.19 \pm 0.09$ ;  $\delta_{\text{cued}}$ :  $z = -1.05$ ,  $p = 0.294$ , Cohen’s  $d = 0.39$ ,  $CI = [-0.15, 0.03]$ ), criteria at the uncued location increased significantly (uncued:  $c_{\text{sham}} = 0.54 \pm 0.08$ ,  $c_{\text{stim}} = 0.64 \pm 0.11$ ;  $\delta_{\text{uncued}}$ :  $z = 2.21$ ,  $p = 0.027$ , Cohen’s  $d = 0.45$ ,  $CI = [-0.03, 0.25]$ ; Fig. 3b). This effect translated into a significant increase in the attentional modulation of criteria ( $\Delta c = c_{\text{cued}} - c_{\text{uncued}}$ ) following cTBS ( $\Delta c_{\text{sham}} = -0.68 \pm 0.12$ ,  $\Delta c_{\text{stim}} = -0.84 \pm 0.12$ ;  $\delta_{\Delta}$ :  $z = -2.60$ ,  $p = 0.009$ , Cohen’s  $d = 0.67$ ,  $CI = [-0.31, -0.03]$ ; Fig. 3d). In other words, rPPC cTBS affected hit rates by reducing the bias (increasing the criterion) for reporting changes at the uncued location. Further insights linking cTBS-induced modulations of psychophysical parameters ( $d'$ ,  $c$ ) with behavioral (psychometric) responses are provided in the SI Results section on *Effects of neurostimulation on mislocalization responses* (Supplementary Fig. S5 and Supplementary Table S1).

We confirmed these results with a two-way ANOVA. While cueing produced a statistically significant main effect on both sensitivity ( $d'$ ,  $F_{1,27} = 29.55$ ,  $p < 0.001$ ) and criterion ( $c$ ,  $F_{1,27} = 44.05$ ,  $p < 0.001$ ),

stimulation did not produce a statistically significant main effect in either case ( $p > 0.1$ ). Nevertheless, we observed a significant interaction between cueing and stimulation condition, only for the criterion ( $F_{1,27} = 6.23$ ,  $p = 0.019$ ) and not for sensitivity ( $F_{1,27} = 0.38$ ,  $p = 0.543$ ). Finally, post-hoc comparisons revealed that stimulation produced a significant increase in the uncued criterion ( $p = 0.031$ , Fishers’ LSD) but no statistically significant effect on the other parameters ( $p > 0.05$ ). We also tested for differential effects of rPPC stimulation in the contralateral versus ipsilateral hemifields using a two-way ANOVA with stimulation condition (sham, stim) and change hemifield (ipsilateral, contralateral). We did not observe any statistically significant effect of laterality (i.e., interaction between stimulation condition and change hemifield) on either parameter ( $d'$ ,  $c$ ) at any location (cued  $d'$ :  $F_{1,27} = 1.31$ ,  $p = 0.263$ ; cued  $c$ :  $F_{1,27} = 0.32$ ,  $p = 0.574$ ; uncued  $d'$ :  $F_{1,27} = 0.83$ ,  $p = 0.369$ ; uncued  $c$ :  $F_{1,27} = 0.00$ ,  $p = 0.986$ ;  $\Delta d'$ :  $F_{1,27} = 1.54$ ,  $p = 0.225$ ;  $\Delta c$ :  $F_{1,27} = 0.13$ ,  $p = 0.724$ ). Finally, we computed the Bayes factors for the sensitivity and criterion effects induced by rPPC cTBS. This analysis revealed moderate evidence for an increase in criterion modulation following cTBS ( $\Delta c$ ,  $BF_{+0} = 5.32$ ) but also moderate evidence for no change in sensitivity modulation ( $\Delta d'$ ,  $BF_{10} = 0.24$ ). A Bayesian sequential analysis robustness check (JASP<sup>31</sup>) – performed by computing Bayes Factors across successive data points acquired – revealed that the trends on

$\Delta d'$  and  $\Delta c$  persisted nearly throughout data collection (Supplementary Fig. S8).

Next, we asked whether rPPC cTBS effects could be better explained by changes in either sensitivity or bias alone, employing formal model comparison analysis<sup>5</sup> (Methods section on *Model comparison analysis*). Briefly, we modified the m-ADC model in two ways to fit the behavioral effects of stimulation: i) a “selective bias-effect” model, in which sensitivity values at each location during the real (stim) cTBS session were constrained to be equal to their corresponding values during the sham cTBS session (Fig. 3e), and ii) a “selective sensitivity-effect” model, in which criterion values at each location during the real (stim) cTBS session were constrained to be equal to their corresponding values during the sham cTBS session (Fig. 3e). Both of these, more parsimonious, models were compared against the standard m-ADC model that incorporated both sensitivity and bias effects (“both-effects” model) using the Bayesian Information Criterion (BIC; Fig. 3f; Methods).

The selective bias-effect model outperformed both the selective sensitivity-effect model (BIC: bias-effect model:  $401.5 \pm 73.8$ , sensitivity-effect model:  $437.3 \pm 72.9$ ;  $\Delta$ BIC (bias-effect – sensitivity-effect):  $z = -4.62$ ,  $p < 0.001$ , signed rank test, Cohen's  $d = 3.24$ ,  $CI = [-41.8, -29.7]$ ; Fig. 3f) and the both-effects model (both-effects model:  $438.3 \pm 70.6$ ;  $\Delta$ BIC (bias-effect – both-effects):  $z = -4.62$ ,  $p < 0.001$ , Cohen's  $d = 5.56$ ,  $CI = [-40.6, -32.9]$ ; Fig. 3f) with significantly lower BIC values. The selective sensitivity-effect model's BIC value was not statistically significantly different from that of the both-effects model ( $\Delta$ BIC (sensitivity-effect – both-effects):  $z = -1.21$ ,  $p = 0.228$ , Cohen's  $d = 0.13$ ,  $CI = [-5.2, 3.2]$ ). Similar results were observed when model comparison was performed with the corrected Akaike Information Criterion (Supplementary Fig. S3c). In other words, model comparison analysis indicated that the effect of rPPC cTBS could be better explained as a change in bias rather than a change in sensitivity.

In summary, rPPC cTBS selectively affected attentional bias modulation. The effect manifested as a statistically significant reduction in the reorienting of spatial choice bias: a decrease in bias (increase in criterion) for reporting changes at the uncued location. By contrast, we observed moderate evidence against an effect of rPPC cTBS on sensitivity modulation. Model evidence from the Bayes factor, as well as model comparison analyses, revealed that stimulation effects could best be explained by a change in bias modulation rather than by a change in sensitivity modulation. The results suggest a specific role for the rPPC in the reorienting of spatial choice bias.

### Effects of 40 Hz rPPC tACS on psychometric responses

We performed an additional set of experiments by perturbing rPPC activity using 40 Hz transcranial alternating current stimulation (tACS) and studying the effect on sensitivity and bias. tACS sessions followed a protocol similar to that of Helfrich et al. (2014)<sup>32</sup> (Methods section on *tACS experiments*)<sup>32</sup>. Briefly, participants ( $n = 26$ ) completed three sessions of the cued attention task (Fig. 1a) comprising 250 trials, lasting 20 min, each (Experiment Protocol in Fig. 1c, right). The first session was always a sham tACS session (“sham” session). Following a brief interval (5 min) after the conclusion of the sham session, we delivered 40 Hz high-definition tACS (peak-to-peak amplitude: 1.5–2.0 mA, Methods) continuously for 20 min over the posterior parietal electrodes in the right hemisphere (“stimulation” session; Supplementary Fig. S2d, e). A third post-stimulation (washout) session was conducted 30 min after the end of the 40 Hz tACS session (“post” session).

For the tACS experiment, sham and stimulation sessions were conducted in a sequential order, rather than in counterbalanced order, for the following reason: Many recent studies<sup>33,34</sup> have shown that the effects of tACS can outlast the stimulation itself by  $>30$  min. Therefore, the sham session was always conducted before the stimulation session, followed by the post-stimulation session to assess whether the effect of 40 Hz tACS stimulation

had “washed out”. If the sham session were conducted after the stimulation session, and if tACS effects were to persist into the former, this would heavily dilute tACS effect sizes. This 3-session tACS design is identical to that adopted in earlier, widely cited studies<sup>32,35</sup>. Because of this sequential ordering of sessions, in addition to comparing behavioral results between the sham and stimulation sessions, behavioral results were also compared between the sham and post sessions to discount training and familiarity effects.

As a preliminary step, we confirmed that participants successfully utilized the cue to increase their hit rates at the cued location across all three sessions ( $\Delta$ HR-sham (cued-uncued):  $z = 4.43$ ,  $p < 0.001$ , Wilcoxon signed rank Test, Cohen's  $d = 2.09$ ,  $CI = [14.7, 26.5]\%$ ;  $\Delta$ HR-stim:  $z = 4.46$ ,  $p < 0.001$ , Cohen's  $d = 3.08$ ,  $CI = [20.0, 30.6]\%$ ;  $\Delta$ HR-post:  $z = 4.46$ ,  $p < 0.001$ , Cohen's  $d = 1.84$ ,  $CI = [13.9, 27.3]\%$ ; Fig. 4a, b, Supplementary Fig. S6a). Following 40 Hz tACS over the rPPC, hit rates at both the cued and the uncued locations did not change statistically significantly (cued: HR-sham =  $63.3 \pm 2.4\%$ , HR-stim =  $64.2 \pm 2.3\%$ ;  $\delta_{\text{cued}}$  (stim-sham):  $z = 1.00$ ,  $p = 0.316$ , signed rank test, Cohen's  $d = 0.24$ ,  $CI = [-1.2, 3.0]\%$ ; Fig. 4a, b; uncued: HR-sham =  $42.7 \pm 3.5\%$ , HR-stim =  $38.9 \pm 3.7\%$ ;  $\delta_{\text{uncued}}$ :  $z = -1.89$ ,  $p = 0.058$ , Cohen's  $d = 0.61$ ,  $CI = [-7.4, -0.2]\%$ ; Fig. 4a, b). Similarly, the attentional modulation of hit rates did not increase statistically significantly following tACS ( $\Delta$ HR-sham =  $20.6 \pm 2.9\%$ ,  $\Delta$ HR-stim =  $25.3 \pm 2.6\%$ ;  $\delta_{\Delta}$ :  $z = 1.89$ ,  $p = 0.058$ , Cohen's  $d = 0.61$ ,  $CI = [0.3, 9.2]\%$ ; Fig. 4e top left). In addition, false alarm rates did not change statistically significantly at any location (Fig. 4d) (cued: FAR-sham =  $14.2 \pm 1.8\%$ , FAR-stim =  $12.1 \pm 1.8\%$ ;  $\delta_{\text{cued}}$ :  $z = -1.60$ ,  $p = 0.109$ , Cohen's  $d = 0.37$ ,  $CI = [-5.3, 1.1]\%$ ; uncued: FAR-sham =  $12.8 \pm 2.3\%$ , FAR-stim =  $14.7 \pm 2.1\%$ ;  $\delta_{\text{uncued}}$ :  $z = 1.79$ ,  $p = 0.074$ , Cohen's  $d = 0.52$ ,  $CI = [-0.2, 4.2]\%$ ). Moreover, attentional modulation of false alarm rates decreased significantly ( $\Delta$ FAR-sham =  $1.4 \pm 2.2\%$ ,  $\Delta$ FAR-stim =  $-2.6 \pm 1.5\%$ ;  $\delta_{\Delta}$ :  $z = -2.40$ ,  $p = 0.016$ , Cohen's  $d = 0.61$ ,  $CI = [-8.0, -0.1]\%$ ) (Fig. 4e bottom).

We also performed a two-way ANOVA, similar to that for the cTBS cohort, to test for the effects of cueing (cued, uncued) and stimulation condition (sham, stim) on the parameters: We observed a statistically significant main effect of cueing only on hit rates ( $F_{1,25} = 84.53$ ,  $p < 0.001$ ) but not on false alarm rates ( $F_{1,25} = 0.14$ ,  $p = 0.715$ ). There was no statistically significant main effect of stimulation condition ( $p > 0.05$  for both HR and FAR), but a significant interaction between cueing and stimulation condition on both metrics (HR:  $F_{1,25} = 4.75$ ,  $p = 0.039$ ; FAR:  $F_{1,25} = 4.51$ ,  $p = 0.044$ ); the effect on HR paralleled those observed with cTBS. In addition, tACS also produced systematic effects on the attentional modulation of mislocalization rates, paralleling those of cTBS (Fig. 4c, e top right); these results are described in the SI Results section on *Effects of neurostimulation on mislocalization responses*.

Furthermore, we tested for differences between the sham and post-stim conditions and observed no statistically significant differences in either psychometric parameter (hit rates and false alarm rates) at either location (cued: HR-post =  $63.9 \pm 2.4\%$ ;  $\delta_{\text{cued}}$  (post-sham):  $z = 0.50$ ,  $p = 0.620$ , Cohen's  $d = 0.15$ ,  $CI = [-1.7, 2.9]\%$ ; uncued: HR-post =  $43.3 \pm 3.8\%$ ;  $\delta_{\text{uncued}}$ :  $z = 0.34$ ,  $p = 0.732$ , Cohen's  $d = 0.12$ ,  $CI = [-2.5, 3.8]\%$ ; cued: FAR-post =  $11.0 \pm 1.7\%$ ;  $\delta_{\text{cued}}$ :  $z = -1.39$ ,  $p = 0.166$ , Cohen's  $d = 0.45$ ,  $CI = [-7.3, 0.9]\%$ ; uncued: FAR-post =  $12.4 \pm 2.2\%$ ;  $\delta_{\text{uncued}}$ :  $z = -0.50$ ,  $p = 0.619$ , Cohen's  $d = 0.08$ ,  $CI = [-3.4, 2.6]\%$ ; Supplementary Fig. S6a-b) or their modulations ( $\Delta$ HR-post =  $20.6 \pm 3.3\%$ ;  $\delta_{\Delta}$ :  $z = 0.04$ ,  $p = 0.970$ , Cohen's  $d < 0.01$ ,  $CI = [-4.1, 4.1]\%$ ;  $\Delta$ FAR-post =  $-1.4 \pm 2.0\%$ ;  $\delta_{\Delta}$ :  $z = -0.93$ ,  $p = 0.354$ , Cohen's  $d = 0.29$ ,  $CI = [-8.3, 2.6]\%$ ; Supplementary Fig. S6c). A two-way ANOVA further revealed no statistically significant interaction between cueing (cued, uncued) and stimulation condition (sham, post) on either parameter (HR:  $F_{1,25} = 0$ ,  $p = 0.998$ ; FAR:  $F_{1,25} = 1.12$ ,  $p = 0.300$ ).

However, reaction times were significantly faster during the stimulation, compared to the sham session, at the cued location (cued:

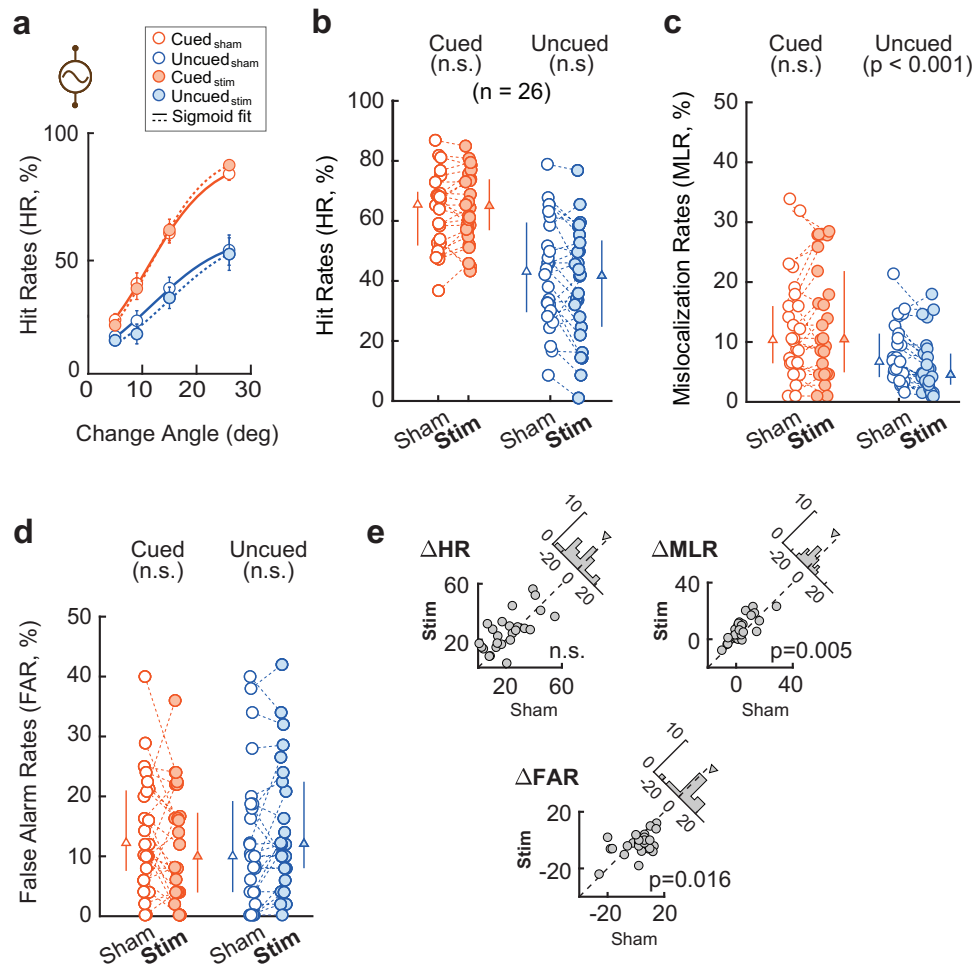


**Fig. 4 | Effects of 40 Hz tACS over rPPC on psychometrics.** **a** Same as in Fig. 2a but showing the psychometric functions of hit rates as a function of orientation change angle magnitude (average across  $n = 26$  participants) during the sham tACS (Sham; open circles) and real tACS (Stim; filled circles) sessions. Other conventions are the same as in Fig. 2a. **b** Same as in Fig. 2b but showing Hit rates (HR) for detecting changes at the cued (orange) and uncued locations (blue) in Sham (open circles) and Stim (filled circles) tACS sessions ( $n = 26$ ), averaged over all angles.  $p$ -values denote statistical significance levels assessed with a two-sided Wilcoxon signed rank test, followed by a Benjamini-Hochberg correction for multiple comparisons.

Other conventions are the same as in Fig. 2b. **c** Same as in panel (b), but showing mislocalization rates (MLR) at the cued (orange) and uncued (blue) locations (tACS). Other conventions are the same as in panel (b). **d** Same as in panel (b), but showing false alarm rates (FAR) at the cued (orange) and uncued (blue) locations (tACS). Other conventions are the same as in panel (b). **e**. Same as in Fig. 2e but showing the attentional modulation of hit rates ( $\Delta HR = HR_{\text{cued}} - HR_{\text{uncued}}$ ; top left), mislocalization rates ( $\Delta MLR = MLR_{\text{cued}} - MLR_{\text{uncued}}$ ; top right) and false alarm rates ( $\Delta FAR = FAR_{\text{cued}} - FAR_{\text{uncued}}$ ; bottom) in the Sham (x axis) and Stim (y axis) tACS sessions ( $n = 26$ ). Other conventions are the same as in Fig. 2e.

RT-sham =  $571 \pm 17$  ms, RT-stim =  $539 \pm 16$  ms;  $\delta_{\text{cued}}$ :  $z = -3.70$ ,  $p < 0.001$ , Cohen's  $d = 1.29$ ,  $CI = [-47, -18]$  ms) but not statistically significantly faster at the uncued location (uncued: RT-sham =  $701 \pm 21$  ms, RT-stim =  $675 \pm 20$  ms;  $\delta_{\text{uncued}}$ :  $z = -1.87$ ,  $p = 0.062$ , signed rank test, Cohen's  $d = 0.41$ ,  $CI = [-66, 7]$  ms; Supplementary Fig. S3b). These effects continued into the post-stimulation session as compared to the sham session at the cued location (cued: RT-post =  $534 \pm 15$  ms;  $\delta_{\Delta}$  (post-sham):  $z = -3.75$ ,  $p < 0.001$ , Cohen's  $d = 1.60$ ,  $CI = [-51, -24]$  ms). The results suggest that tACS effects on reaction times could perhaps be explained by training effects.

In summary, 40 Hz tACS over the rPPC produced effects on hit rates and mislocalization responses that qualitatively paralleled the effects of rPPC cTBS. We next tested for the effects of 40 Hz rPPC tACS on the psychophysical parameters.

#### Effects of 40 Hz rPPC tACS on sensitivity and bias

Next, we examined the effects of 40 Hz tACS over rPPC on sensitivity and bias. In line with the cTBS results, rPPC tACS produced no statistically significant effects on  $d'$ , either at the cued location (cued:  $d'$

sham =  $1.74 \pm 0.10$ ,  $d'$ -stim =  $1.87 \pm 0.10$ ;  $\delta_{\text{cued}}$  (stim-sham):  $z = 1.51$ ,  $p = 0.131$ , Cohen's  $d = 0.43$ ,  $CI = [-0.04, 0.31]$ ) or at the uncued location (uncued:  $d'$ -sham =  $1.03 \pm 0.10$ ,  $d'$ -stim =  $0.95 \pm 0.10$ ;  $\delta_{\text{uncued}}$ :  $z = -1.16$ ,  $p = 0.248$ , Cohen's  $d = 0.34$ ,  $CI = [-0.22, 0.06]$ ; Fig. 5a). Nor did tACS produce a statistically significant effect on the attentional modulation of  $d'$  ( $\Delta d'$ -sham =  $0.71 \pm 0.08$ ,  $\Delta d'$ -stim =  $0.92 \pm 0.11$ ;  $\delta_{\Delta}$ :  $z = 1.77$ ,  $p = 0.078$ , signed rank test; Cohen's  $d = 0.54$ ,  $CI = [-0.02, 0.44]$ ; Fig. 5c). Similar to cTBS, we further analyzed the entire psychophysical function ( $d'$  as a function of change angle; Supplementary Fig. S4b): A two-way ANOVA revealed no statistically significant interaction between stimulus strength (change angle values, i.e.,  $\Delta\theta$ ) and stimulation condition on  $\Delta d'$  ( $F_{1,100} = 1.28$ ,  $p = 0.283$ ).

In contrast, tACS produced systematic effects on criteria: Criteria at the cued location were not statistically significantly different (cued: c-sham =  $0.20 \pm 0.09$ , c-stim =  $0.20 \pm 0.10$ ;  $\delta_{\text{cued}}$ :  $z = -0.06$ ,  $p = 0.949$ , Cohen's  $d = 0.05$ ,  $CI = [-0.09, 0.10]$ ), whereas criteria at the uncued location increased significantly (uncued: c-sham =  $0.58 \pm 0.10$ , c-stim =  $0.70 \pm 0.12$ ;  $\delta_{\text{uncued}}$ :  $z = 2.48$ ,  $p = 0.013$ , Cohen's  $d = 0.86$ ,  $CI = [0.04, 0.22]$ ; Fig. 5b). As a consequence, this yielded a significant increase in the attentional modulation of criteria following tACS ( $\Delta c$

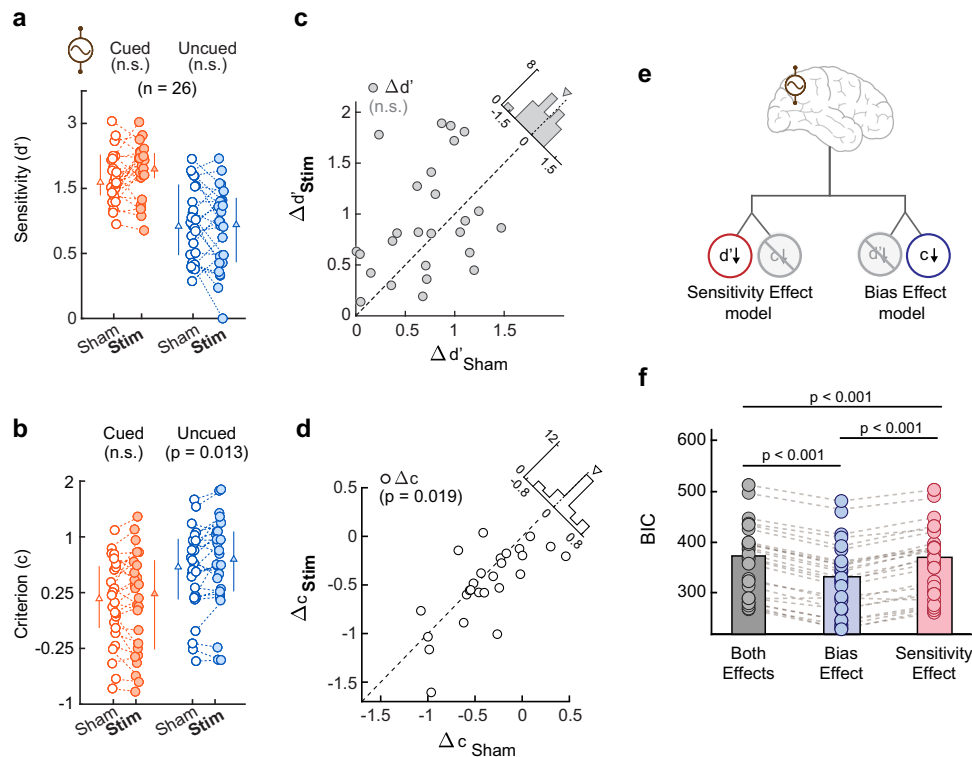


**Fig. 5 | Effects of 40 Hz tACS over rPPC on sensitivity and bias.** **a** Same as in Fig. 3a, but for the Sham (open circles) and Stim tACS (filled circles) sessions ( $n = 26$  participants).  $p$ -values denote statistical significance levels assessed with a two-sided Wilcoxon signed rank test, followed by a Benjamini-Hochberg correction for multiple comparisons. Other conventions are the same as in Fig. 3a. **b** Same as in panel (a), but for criterion. Other conventions are the same as in Fig. 3b. **c** Same as Fig. 3c but showing the attentional modulation of sensitivity ( $\Delta d' = d'_{\text{cued}} - d'_{\text{uncued}}$ ; grey circles) in the Sham ( $x$  axis) and Stim ( $y$  axis) tACS sessions. (Top right inset)

Histogram of  $\Delta d'$  values across participants ( $n = 26$ ). Other conventions are the same as in Fig. 3c. **d** Same as in panel (c), but for criterion ( $\Delta c = c_{\text{cued}} - c_{\text{uncued}}$ ; open circles). Other conventions are the same as in Fig. 3d. **e** Schematic of model comparison analysis for rPPC tACS stimulation effects. Other conventions are the same as in Fig. 3e. **f** Same as in Fig. 3f but showing the mean Bayesian Information Criterion (BIC) scores for the both-effects (grey), bias-effect (blue) and sensitivity-effect (red) models for the tACS cohort ( $n = 26$ ). Other conventions are the same as in Fig. 3f.

sham =  $-0.38 \pm 0.08$ ,  $\Delta c$ -stim =  $-0.50 \pm 0.08$ ;  $\delta_{\Delta}$ :  $z = -2.35$ ,  $p = 0.019$ , Cohen's  $d = 0.56$ ,  $CI = [-0.24, 0.00]$ ; Fig. 5d). Further insights linking tACS-induced modulations of psychophysical parameters ( $d'$ ,  $c$ ) with behavioral (psychometric) responses are provided in the SI Results section on *Effects of neurostimulation on mislocalization responses* (Supplementary Fig. S5 and Supplementary Table S1). Again, as with the cTBS cohort, we performed a two-way ANOVA to test the effects of cueing (cued, uncued) and stimulation condition (sham, stim) on the parameters. We observed a statistically significant main effect of cueing on both sensitivity ( $d'$ ,  $F_{1,25} = 115.82$ ,  $p < 0.001$ ) and criterion ( $c$ ,  $F_{1,25} = 38.4$ ,  $p < 0.001$ ), but no statistically significant main effect of stimulation condition in either case ( $p > 0.05$ ); the interaction between cueing and stimulation condition trended toward significance for criterion modulations ( $F_{1,25} = 4.05$ ,  $p = 0.055$ ). Post-hoc comparisons showed a significant increase in the uncued criterion following stimulation ( $p = 0.005$ ); other parameter pairs (cued  $c$ , cued  $d'$  or uncued  $d'$ ) were not statistically significantly different ( $p > 0.05$ ). A two-way ANOVA to test the effects of stimulation condition (sham, stim) and change hemifield (ipsilateral, contralateral) also revealed no statistically significant interaction effect of laterality, either at the cued or uncued locations (cued  $d'$ :  $F_{1,25} = 1.22$ ,  $p = 0.279$ ; cued  $c$ :  $F_{1,25} = 0.00$ ,  $p = 0.988$ ; uncued  $d'$ :  $F_{1,25} = 0.07$ ,  $p = 0.797$ ; uncued  $c$ :  $F_{1,25} = 0.07$ ,  $p = 0.797$ ;  $\Delta d'$ :  $F_{1,25} = 0.62$ ,  $p = 0.438$ ;  $\Delta c$ :  $F_{1,25} = 0.06$ ,  $p = 0.810$ ). Again, as with the cTBS experiment, we computed Bayes factors for the sensitivity and criterion effects induced by rPPC 40 Hz tACS. This analysis revealed anecdotal evidence for an increase in criterion modulation ( $\Delta c$ ,  $BF_{+0} = 2.27$ ), accompanied by strong evidence favoring an increase in uncued criterion (uncued  $c$ ,  $BF_{-0} = 11.45$ ). By

contrast, there was no evidence for or against a change in sensitivity modulation ( $\Delta d'$ ,  $BF_{10} = 1.01$ ) following tACS. A Bayesian sequential analysis robustness check revealed that the trend on uncued criterion persisted nearly throughout data collection (Supplementary Fig. S9).

As with the psychometric parameters, we tested for differences between the sham and post-stim conditions and observed no statistically significant differences in the attentional modulation of the parameters ( $\Delta d'$ -post -  $\Delta d'$ -sham:  $z = 1.26$ ,  $p = 0.209$ , signed rank test; Cohen's  $d = 0.25$ ,  $CI = [-0.14, 0.36]$ ;  $\Delta c$ -post -  $\Delta c$ -sham:  $z = -0.19$ ,  $p = 0.849$ , Cohen's  $d = 0.08$ ,  $CI = [-0.17, 0.13]$ ; Supplementary Fig. S6d-f). A two-way ANOVA further revealed no statistically significant interaction between cueing (cued, uncued) and stimulation condition (sham, post) on either parameter ( $d'$ :  $F_{1,25} = 0.08$ ,  $p = 0.777$ ;  $c$ :  $F_{1,25} = 0.83$ ,  $p = 0.372$ ). Finally, Bayes factor analysis showed moderate evidence for no difference in the attentional modulation of either sensitivity ( $BF_{10} = 0.30$ ) or criterion ( $BF_{10} = 0.21$ ) across the sham and post sessions.

Next, we tested whether rPPC 40 Hz tACS effects could be better explained by sensitivity or bias changes alone, by comparing the same set of 3 models as before ("selective bias-effect", "selective sensitivity-effect" and "both effects"). Again, the selective bias-effect model outperformed both the selective sensitivity-effect model (BIC: bias-effect model:  $325.7 \pm 69.6$ , sensitivity-effect model:  $357.0 \pm 70.4$ ;  $\Delta BIC$  (bias-effect - sensitivity-effect):  $z = -4.43$ ,  $p < 0.001$ , Cohen's  $d = 4.35$ ,  $CI = [-35.4, -27.1]$ ; Fig. 5e) and the both-effects model (both-effects model:  $362.7 \pm 70.4$ ;  $\Delta BIC$  (bias-effect - both-effects):  $z = -4.43$ ,  $p < 0.001$ , Cohen's  $d = 5.11$ ,  $CI = [-41.1, -32.8]$ ; Fig. 5e; for AICc, see Supplementary Fig. S3d). In other words, bias changes, rather than sensitivity changes, best explained the effects of 40 Hz tACS over rPPC.



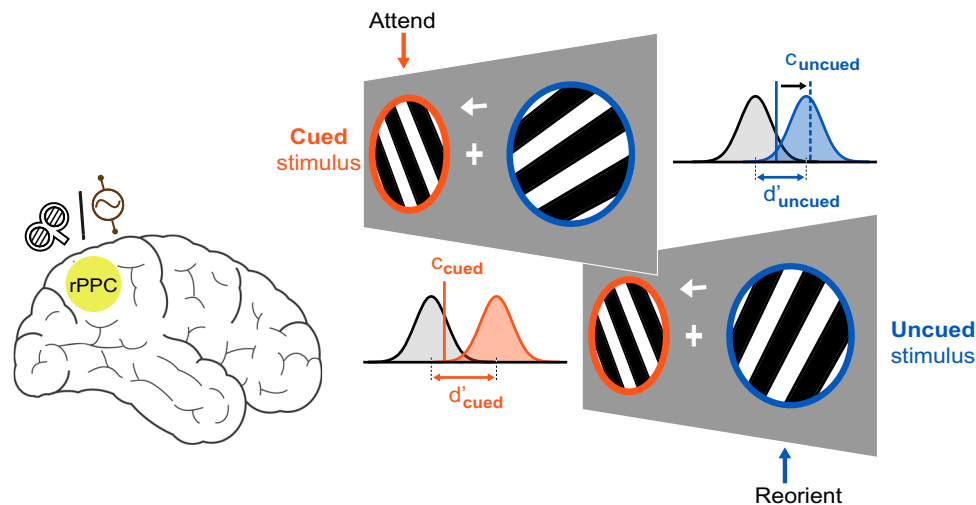


**Fig. 6 | Schematic of rPPC neurostimulation effects on attention components.** Perturbing rPPC activity either with continuous theta-burst stimulation (ctBS) or with 40 Hz transcranial alternating current stimulation (tACS) produces

selective deficits with reorienting spatial choice bias toward the uncued location (increase in  $c_{\text{uncued}}$ ), one specific component of attention.

We conducted a control experiment to test if these effects of rPPC tACS were specific to the 40 Hz frequency (Methods section on *tACS Experiments: Control Experiment*). In this control experiment, we tested an alternative frequency of tACS stimulation (60 Hz) over the right PPC. The number of participants in the control experiment ( $n = 26$ ) was identical to that of the main experiment (Supplementary Fig. S7).

60 Hz tACS produced no statistically significant effects on  $d'$ , either at the cued location (cued:  $d'$ -sham =  $1.30 \pm 0.10$ ,  $d'$ -stim =  $1.35 \pm 0.09$ ;  $\delta_{\text{cued}}$ :  $z = 0.34$ ,  $p = 0.732$ , Cohen's  $d = 0.19$ ,  $CI = [-0.10, 0.20]$ ) or at the uncued location (uncued:  $d'$ -sham =  $0.75 \pm 0.08$ ,  $d'$ -stim =  $0.78 \pm 0.09$ ;  $\delta_{\text{uncued}}$ :  $z = 0.47$ ,  $p = 0.638$ , Cohen's  $d = 0.14$ ,  $CI = [-0.09, 0.15]$ ). Moreover, attentional modulation of sensitivity was not statistically significantly different following 60 Hz tACS ( $\Delta d'$ -sham =  $0.55 \pm 0.13$ ,  $\Delta d'$ -stim =  $0.58 \pm 0.11$ ;  $\delta_{\Delta}$ :  $z = 0.42$ ,  $p = 0.675$ , Cohen's  $d = 0.06$ ,  $CI = [-0.19, 0.23]$ ) (Supplementary Fig. S7b). Similarly, criterion was not statistically significantly affected at either the cued (cued:  $c$ -sham =  $-0.00 \pm 0.09$ ,  $c$ -stim =  $-0.06 \pm 0.11$ ;  $\delta_{\text{cued}}$ :  $z = -0.98$ ,  $p = 0.328$ , Cohen's  $d = 0.31$ ,  $CI = [-0.16, 0.05]$ ) or the uncued (uncued:  $c$ -sham =  $0.48 \pm 0.08$ ,  $c$ -stim =  $0.52 \pm 0.09$ ;  $\delta_{\text{uncued}}$ :  $z = 0.85$ ,  $p = 0.395$ , Cohen's  $d = 0.16$ ,  $CI = [-0.09, 0.15]$ ) locations, again, yielding no statistically significant modulation of criterion with 60 Hz tACS ( $\Delta c$ -sham =  $-0.49 \pm 0.11$ ,  $\Delta c$ -stim =  $-0.57 \pm 0.12$ ;  $\delta_{\Delta}$ :  $z = -1.46$ ,  $p = 0.144$ , Cohen's  $d = 0.33$ ,  $CI = [-0.24, 0.06]$ ) (Supplementary Fig. S7c). Bayes factors revealed moderate evidence for no change in either criterion modulation ( $\Delta c$ ,  $BF_{10} = 0.31$ ) or sensitivity modulation ( $\Delta d'$ ,  $BF_{10} = 0.21$ ) following control 60 Hz tACS. Additional control analyses, to account for inter-individual variations in performance, are reported in SI Results.

In summary, 40 Hz tACS over rPPC affected hit rates by reducing the bias (increasing the criterion) for reporting changes at the uncued location. Model comparison analysis confirmed that tACS effects were best explained by a model that incorporated only bias changes. A control experiment indicated that 40 Hz stimulation effects were frequency-specific and could not be explained by training or familiarity effects.

In addition, to test if neurostimulation effects on  $d'$  and criterion were robust to assumptions in the m-ADC model, we also analyzed participants' behavior with a similarity choice model; this analysis revealed converging evidence for a consistent effect of stimulation on criterion modulation ( $\Delta c$ ), but not on sensitivity modulation ( $\Delta d'$ ) (see SI Results on *Analysis with a similarity choice model*).

Taken together, the results of both experiments demonstrate that: i) rPPC stimulation produced systematic and robust effects on

choice bias; evidence for sensitivity effects was either lacking (ctBS) or equivocal (tACS); ii) both inhibitory theta burst stimulation (ctBS) and 40 Hz tACS produced a significant reduction in choice bias (increase in criterion) at the uncued location; iii) as a result, both stimulation modalities strongly increased the attentional cueing-induced modulation of choice bias (Fig. 6). These results indicate that the rPPC plays a causal role in reorienting one specific component of attention – spatial choice bias.

## Discussion

The posterior parietal cortex (PPC) is associated with multiple sensory, motor, and cognitive functions<sup>10,11,36</sup>. Activations of the dorsal PPC, in particular, the intraparietal sulcus and superior parietal lobule (IPS/SPL; BA 7), are consistently observed in attention tasks, marking these regions as key nodes of the dorsal frontoparietal attention network in the forebrain<sup>11</sup>. Here, we investigated the causal role of the dorsal rPPC with two neurostimulation modalities – inhibitory theta burst stimulation (ctBS) and 40 Hz transcranial alternating current stimulation (tACS) – and, using a recent signal detection model<sup>25</sup>, quantified the effects on distinct components of attention – sensitivity and bias. Our results suggest a specific role for the dorsal rPPC in reorienting bias toward the uncued location.

## Methodological limitations and controls

The multialternative (m-ADC) task in this study employs spatial probabilistic cueing. This task derives from an endogenously cued version of the classic Posner cueing paradigm<sup>19</sup>: a canonical attentional task widely employed in literature to measure attention's effects on neurons and behavior<sup>4,37,38</sup>. Yet, previous studies have suggested that such a task conflates the effect of spatial attention and spatial expectation<sup>39,40</sup>. For example, a study by Wyart et al. (2012)<sup>39</sup> employed a two-alternative forced choice (2-AFC) task and showed that signal relevance modulated sensitivity but not criterion. Similarly, Tarasi et al. (2022)<sup>40</sup> elegantly demonstrated that varying signal expectation modulated criterion, but not sensitivity, and identified its neural correlates.

By contrast, several recent studies have shown that – unlike the 2-AFC task – both sensitivities and criteria are modulated by attentional mechanisms in m-ADC tasks<sup>4–6</sup>. Specifically, a recent study<sup>5</sup> applied novel risk curvature analyses to show that m-ADC criteria quantify the weighting of sensory evidence across locations, and are linked to attentional selection, rather than expectation, mechanisms.

Importantly, these findings have been replicated, and the m-ADC model validated, by many subsequent studies<sup>6,25,26,30,41</sup>. Consequently, in the present study also, m-ADC criterion modulations induced by spatial probabilistic cueing and the effects of rPPC stimulation likely reflect attentional mechanisms. Combining neural recordings (e.g., electroencephalography or functional MRI) with neurostimulation could provide further evidence by identifying the effects of rPPC stimulation on specific neural signatures of attentional modulation<sup>42</sup>.

Despite being widely-used, state-of-the-art techniques for non-invasive perturbation of human brain activity, both TMS and tACS suffer from key limitations: TMS neurostimulation effects have a spatial spread of ~1 cm radius<sup>43,44</sup> whereas the effects of high-density tACS neurostimulation occur over even larger areas (~4 cm), determined by the spatial configuration of the electrodes<sup>45</sup>. Our cTBS pulses were targeted toward the intraparietal sulcus (third functional subdivision; Supplementary Fig. S2a), and tACS was applied with an electrode montage centered at the P4 electrode (Supplementary Fig. S2d, e). Nonetheless, the potential for the spatial spread of induced activity – either directly, through volume conduction or indirectly, through synaptic transmission – renders it challenging to localize the functional consequences of neurostimulation in this study to particular sub-divisions within the PPC. Nonetheless, both stimulation paradigms produced a consistent pattern of deficits with reorienting choice bias.

In our cTBS experiment, sham stimulation was conducted by holding the coil orthogonal to the target site rather than with vertex or placebo stimulation. Several reasons necessitated this choice. First, TMS-fMRI studies have shown that vertex stimulation results in the deactivation of several brain areas associated with the default mode network (DMN)<sup>44</sup>. Some sites within the PPC show overlap with the DMN<sup>44</sup> and we sought to avoid these unforeseen interactions. Second, modelling studies<sup>43</sup> have shown that cTBS of the vertex may lead to activation of adjacent cortical motor sites like the supplementary motor area (SMA), which could yield unexpected effects on response times. Moreover, other brain areas functionally linked with regions proximal to the vertex (e.g., SMA, paracentral lobule) may also be affected by vertex stimulation<sup>43</sup>. Finally, cTBS is an offline stimulation protocol. Compared to an online protocol – in which TMS-evoked auditory or somatic sensations can affect task performance due to concurrent stimulation – in an offline protocol, such a concern is substantially ameliorated because no TMS is delivered during the actual task.

In our tACS experiment, sham stimulation was conducted by ramping on and off the current for the first and last 30 s of the 20 min sham control<sup>32,46</sup>. A mild tingling sensation occurs primarily during the ramping phase of the current, and the sham protocol we employed here has been widely used to control for this sensation<sup>32,35,46</sup>. Alternatively, we could have also applied active stimulation over other cortical areas (e.g., frontal eye field, FEF). Yet, the results of this latter control experiment would not be easily interpretable. For example, if the FEF were functionally coupled with the PPC during attention, FEF tACS may yield similar effects on uncued criteria (or it may not). The results of such an experiment would not confirm or invalidate our findings regarding the role of the rPPC. Moreover, in our tACS experiments, the stimulation always followed the sham session to avoid carryover effects of the stimulation from leaking into the sham session. Yet, this design raises the concern that behavioral effects in the real stimulation session could be due to learning or familiarity. We addressed this concern by showing that performance returned to the sham baseline in a post stimulation session and also with a control experimental session ( $n = 26$ ) with a design virtually identical with the main experiment. This control experiment confirmed that other frequencies of stimulation (60 Hz tACS) did not reproduce the effect of 40 Hz tACS over the rPPC.

Despite these potential shortcomings, both stimulation modalities produced specific – and nearly identical – effects on uncued

criteria following rPPC stimulation. In other words, converging results from both cTBS and tACS experiments indicate a causal role of the rPPC in reorienting attentional resources, especially when task-relevant events occur at the unattended location. Moreover, they indicate that the rPPC plays a specific role in reorienting spatial choice bias toward the uncued location.

### Putative mechanisms underlying neurostimulation effects

TMS employs the principles of electromagnetic induction to interfere with the neural activity of the stimulated brain area<sup>43</sup>. Numerous studies have demonstrated that continuous theta burst stimulation over the motor cortex induces lasting inhibition of cortical excitability<sup>22,47,48</sup>. This suppression has been linked to neuroplasticity mechanisms. Specifically, cTBS has been shown to modulate calcium ion influx through the NMDA receptors of cortical pyramidal neurons, thereby decreasing their excitability<sup>48</sup>. Continuous, high frequency stimulation also facilitates GABA-ergic activity of inhibitory interneurons over time, leading to lasting, suppressive effects at the synapse (e.g. long-term depression/LTD)<sup>47,48</sup>. As a consequence, inhibitory effects of cTBS persist, typically, for several tens of minutes to an hour. Studies combining cTBS with functional neuroimaging (fMRI) have also corroborated the inhibitory effect of cTBS. For example, cTBS induces suppression of cortical activity of stimulated regions, like the FEF<sup>29</sup>, and also degrades resting state connectivity between early visual areas<sup>49</sup>. Furthermore, we independently confirmed in a small cohort ( $n = 7$ ) of participants that cTBS indeed produced an inhibitory effect on the motor cortex, as observed by a significant drop in MEP amplitudes that lasted for at least 50 min following stimulation.

Meanwhile, tACS is hypothesized to entrain endogenous oscillations of cortical pyramidal neurons and inhibitory interneurons to the frequency of stimulation<sup>50,51</sup>. In addition, emerging evidence suggests that tACS induces synaptic changes via spike timing dependent plasticity (STDP) mechanisms, which can outlast the stimulation by up to an hour<sup>34,52–54</sup>. For instance,  $\alpha$ -tACS over bilateral occipito-parietal cortex found a persistent alpha enhancement tens of minutes after cessation of tACS, suggesting neuroplasticity at play<sup>53</sup>. Similarly, gamma tACS significantly prolonged the effects of iTBS (intermittent theta burst stimulation) over the right primary motor cortex<sup>54</sup>. While the effects of tACS on neural activity can vary depending on the stimulation frequency<sup>46</sup> and intensity<sup>55</sup>, we hypothesized that 40 Hz tACS would induce a suppressive effect on cortical activity based on prevalent literature.

On the one hand, facilitatory effects of 40 Hz tACS on attentional processes have been observed in a handful of studies<sup>56,57</sup>; other studies have shown inconsistent effects<sup>46,58</sup>. Hoy et al. (2015)<sup>57</sup> observed that 40 Hz tACS over the left DLPFC enhanced target discriminability during a working memory task<sup>57</sup>, while Hopfinger et al. (2017)<sup>56</sup> reported enhanced reaction times following 40 Hz tACS over the right parietal lobe<sup>56</sup>. On the other hand, Laczó et al. (2012) observed no effect of 40 Hz tACS, over the primary visual cortex, on contrast sensitivity during a covert attention task<sup>46</sup>. Similarly, Pahor et al. (2018)<sup>58</sup> reported no effect of 40 Hz tACS - over the bilateral frontal, parietal or fronto-parietal regions across different experiments - on accuracy and reaction times during a working memory task. Importantly, these studies did not distinguish the effects of stimulation on psychophysical parameters like  $d'$  and criteria.

On the other hand, many more studies have shown suppression of neural activity as well as behavioral performance following gamma frequency tACS. For example, tACS at 40 Hz over the primary motor cortex during a serial search task reduced motor excitability and MEP amplitudes and increased reaction times<sup>23</sup>; the authors speculated that a disruptive effect of 40 Hz tACS could arise from an increase in neural gamma-band activity over and above what is normally prevalent in the neocortex. In another study on the motor cortex, tACS at 75 Hz decreased cortical motor excitability and increased short interval

intracortical inhibition<sup>59</sup>. Similarly, applying gamma (40 Hz) tACS over the medial parietal cortex and precuneus in patients with cognitive impairments increased short-latency inhibition<sup>24</sup>. 40 Hz tACS over the auditory cortex reduced perceptual accuracy during a categorization task<sup>60</sup>. Interestingly, a gamma band (47 Hz) tACS over the left occipitoparietal region during an endogenous attention task significantly increased reaction time for only the invalidly cued trials<sup>61</sup>, reflecting a specific effect on reorienting attention. Taken together with these studies, our findings show that 40 Hz tACS disrupted reorienting of one specific component of attention -- choice bias -- likely via functional inhibition of the rPPC.

Such a mechanism appears at odds with recent studies, which have shown a selective relationship between gamma oscillations and feedforward (bottom-up) processing of stimuli in the neocortex; such activity is generally thought to be excitatory in nature<sup>62</sup>. Yet, evidence from optogenetic studies investigating the temporal response characteristics of interneurons suggests a specific role for 40 Hz input in mediating neocortical inhibition. A seminal study showed that 40 Hz optogenetic stimulation selectively activates parvalbumin-positive (PV+) inhibitory interneurons, one of the major interneuron classes in the neocortex<sup>63</sup>. The gain of the PV+ inhibitory neurons' response died away sharply as the stimulation frequency deviated from 40 Hz, indicating frequency-specific, resonant responses. More recent work in Alzheimer's Disease (AD) mouse models has shown that both optogenetically driving PV+ interneurons at 40 Hz or simply optic (visual light) stimulation at 40 Hz reduces amyloid load, an effect that is hypothesized to be mediated by neocortical inhibition induced by 40 Hz stimulation<sup>64</sup>. This finding has been subsequently tested and partially replicated with 40 Hz tACS in human AD patients<sup>65</sup>. In the context of these studies, our findings suggest that 40 Hz tACS produces functional inhibition of the neocortex and motivate further exploration of neural mechanisms underlying these tACS effects.

### The role of the dorsal rPPC in reorienting attention toward task-relevant targets

Distinct sub-divisions within the right dorsal PPC mediate orienting or reorienting of spatial attention depending on task context<sup>15,17,18</sup>. With cTBS, we targeted the right IPS based on extensive correlative and causal evidence for its involvement in spatial attention<sup>1</sup>. The parietal nodes of the dorsal attention network, including the SPL, have been suggested to be involved in reorienting toward salient but task-irrelevant distractors<sup>17,18</sup>. Yet, a seminal study observed greater activation in the dorsal PPC when attention was reoriented to task-relevant targets at the invalidly cued location<sup>66</sup>. Interestingly, the spatial coordinates of the activation peak reported in this study nearly overlaps our own TMS target coordinates. In other words, there is converging evidence for the involvement of dorsal attention network nodes in the right PPC in controlling reorienting spatial attention toward task-relevant targets<sup>67</sup>.

Other neurostimulation studies offer converging evidence for this hypothesis. Several studies applying neurostimulation to the dorsal rPPC have found attentional effects, specifically at the invalidly cued target locations<sup>68,69</sup>. Moreover, during conjunction search, TMS of the PPC produced systematic behavioral effects primarily when the conjunction target was presented at an unfamiliar or unexpected location, which required reorienting of attention to these locations<sup>70</sup>. Similarly, a recent study showed that 40 Hz tACS over the right parietal cortex modulated uncued target detection during an endogenous attention task<sup>56</sup>. Finally, human patients with lesions to the right PPC (IPS) exhibit selective deficits with reorienting attention back to locations with low target probability during visual search<sup>11</sup>. These studies further confirm a causal role for the dorsal rPPC in reorienting attention toward task-relevant targets.

Interestingly, we observed no significant effects of dorsal rPPC stimulation -- either sensitivity or criterion -- at the cued location. It is

possible that rPPC stimulation may affect cued performance in more challenging attention paradigms or may affect subtler aspects of behavior, such as stimulus or response-history dependence<sup>71</sup>, at the cued location. It is also possible that other key regions of the forebrain attention network (e.g., the FEF) may have compensated for attentional orienting toward the cued location. This hypothesis can be tested in future studies by combining neurostimulation with neuroimaging (e.g., concurrent TMS-fMRI<sup>72</sup> or tACS-fMRI<sup>73</sup>).

We did not observe strong evidence for lateralized effects with either rPPC cTBS or 40 Hz tACS. Classical studies documenting lesions of the right PPC report characteristic, contralesional (left) hemispatial neglect<sup>14,74</sup>. However, other studies have reported evidence of bilateral effects also. For example, patients with right intraparietal lobule (IPL) lesions showed a decrease in contralesional extinction when presented with bilateral stimuli that elicited Gestalt percepts (e.g., Kanizsa stimuli<sup>75</sup>) or in tasks that required parallel visual processing across the hemifields<sup>76</sup>. There is considerable evidence for right hemispheric dominance for visuospatial attention in humans, especially when the stimulus is infrequent or invalidly cued<sup>1,77</sup>. In fact, recent studies have suggested that visuospatial functions are controlled by right hemispheric nodes of the dorsal fronto-parietal attention network, with the left hemispheric nodes involved in non-spatial and motor attention<sup>20</sup>.

Multiple studies have provided evidence suggesting that dorsal rPPC nodes control attention bilaterally across hemifields. For example, an rTMS study targeting the right SPL reported bilaterally impaired target discrimination following stimulation<sup>78</sup>. Similarly, BOLD responses in the right IPS showed no significant evidence of laterality during a change detection task<sup>79</sup>. Moreover, even in lesion studies, although one IPS-lesion patient (H.H) showed a strong contralesional deficit in invalidly cued trials, the other patient (N.V.), whose lesion extended to the superior parietal lobule, showed a bilateral deficit<sup>67</sup>. Given that rPPC lesion patients tested in such experiments have had some time to recover, left hemispheric compensatory mechanisms may have developed, thereby manifesting a strongly lateralized effect. On the other hand, it is possible that the acute functional inhibition of rPPC with cTBS or tACS in our study did not provide a window long enough for left hemispheric compensation to occur, thereby yielding a bilateral effect.

### Distinguishing the rPPC's contribution to sensitivity versus bias control

We observed a significant and consistent effect of rPPC stimulation on choice bias rather than sensitivity. Our results are consistent with previous observations regarding the role of the PPC in encoding decision states and biasing choices based on reward and choice histories<sup>80,81</sup>. Moreover, microstimulation of the LIP produced an increase in the proportion of saccadic choices toward the stimulated neurons' receptive field<sup>82</sup>.

Our findings are also relevant for understanding the nature of top-down influences exerted by PPC over visual cortex, in terms of sensitivity versus bias changes<sup>10,72</sup>. For example, stimulus representations in category-selective regions of ventral temporal cortex systematically vary with the level of activity in the intraparietal sulcus (IPS)<sup>83</sup>. Stimulation of the PPC with single pulse or repetitive TMS increased neuronal activity and excitability in spatially aligned receptive fields in extrastriate visual cortex<sup>1,12,72</sup>. In addition, TMS to the rPPC reduced phosphene thresholds in the visual cortex (area V4) by increasing the excitability of visual cortical neurons<sup>84</sup>. Yet, these influences of PPC on visual cortex are consistent with both sensitivity and bias effects. For example, in a signal detection theory framework, scaling up visual cortex activity for both signal and noise distributions is equivalent to a shift in decision criteria<sup>85</sup>. In a recent study, Di Luzio et al. (2022)<sup>86</sup> showed that cortico-cortical paired associative TMS (ccPAS) between dorsal parietal (IPS/LIP) and visual cortical (V1/V2) regions, during a motion coherence discrimination task, selectively



affected metacognitive decision confidence rather than perceptual sensitivity<sup>86</sup>. This dissociation is consistent with our findings, which show that rPPC stimulation affected decisional weightage (bias) rather than perceptual sensitivity in an endogenous spatial attention task.

Of particular interest are two recent studies that inactivated neural populations in macaque LIP<sup>87,88</sup> and studied the effects on sensitivity and bias. One study found that despite observing robust sensory evidence accumulation signals in LIP neurons, inactivation of these neurons produced no systematic deficits in either sensitivity or bias during task performance<sup>87</sup>. By contrast, LIP inactivation produced a reduction in contralateral choice bias in a free-choice saccade task. On the other hand, the second study<sup>88</sup> reported systematic effects of LIP inactivation on both sensitivity (threshold) and bias parameters. Interestingly, sensitivity impairments occurred only when the visual motion stimulus was placed within the inactivated visual field, whereas choice bias impairments occurred as long as a saccade had to be executed to a target within the inactivated visual field. In other words, PPC inactivation produced robust effects on both sensitivity and bias contralateral to the inactivated location. In our study, neither cTBS nor tACS over human rPPC produced any effects on sensitivity. Moreover, they produced an effect, selectively, on reorienting spatial choice bias, consistent with the vast body of literature on the human rPPC<sup>10,15,17,18</sup>. In addition to direct explanations in terms of inter-species differences, it is possible that differences in stimulus (motion stimuli versus gratings) or response modalities (saccades versus button press responses) could explain the discrepancies with these previous studies. Integrating evidence from studies with diverse stimulus types and sensorimotor mappings will be key to understanding the causal role of the PPC in controlling endogenous visual attention.

## Methods

### Participant details

A total of 88 participants (83 unique individuals, including 26 females) with no known history of neurological or psychological disorders, and with normal or corrected to normal vision were tested in the two experiments. All participants provided written, informed consent and underwent questionnaire-based screening for contra-indications to stimulation. All experimental procedures were approved by the Institute Human Ethics Committee at the Indian Institute of Science, Bangalore.

De-identified individual data has been made available to reproduce the results<sup>89</sup> (see Data Availability). The sex and gender of the participants were self-reported. Because our aims do not include comparative analyses based on the sex or gender of the participants, this information has not been considered in the design of this study.

**cTBS experiments.** 36 healthy participants (14 females, age range 19–35 years; median age 22 years) participated in the continuous theta burst stimulation (cTBS) experiments. Of these, 28 participated in the rPPC cTBS experiment and 8 in the motor cortex cTBS experiment. There was no overlap between the rPPC and motor cortex cTBS participants. All participants but one in the rPPC cohort were right-handed. Data from 1 participant in the motor cortex cTBS experiment was excluded from further analyses due to head twitches.

**tACS experiments.** 52 healthy participants (12 females, age range 18–35 years; median age 23 years) participated in the transcranial alternating current stimulation (tACS) experiments. Of these, 26 participated in the main 40 Hz rPPC stimulation experiment (main cohort), and the remaining 26 participated in a control 60 Hz rPPC stimulation experiment (control cohort). All participants were right-handed. In the main cohort, each participant participated in two tACS experiments – one for the left PPC stimulation and one for the right PPC stimulation. These experiments occurred on different days (counterbalanced order) and were separated by at least one week (see

also SI Results section on *Additional control analyses for training and session order effects*). To enable a direct comparison with the cTBS experiment, we analyze and report results only from the right PPC 40 Hz tACS sessions; results from left PPC tACS sessions are being compiled for a different study. In the control experiment, 3 of the participants also underwent a 60 Hz stimulation session over the left PPC on a different day, separated by at least one week from the rPPC session; the remaining 23 participants underwent only rPPC stimulation. 5 participants overlapped between the cTBS and tACS experiments.

### Experimental procedure: cTBS experiments

**Neuro-navigation protocol.** For precise positioning of the TMS coil, the rPPC was localized with a frameless stereotaxic neuro-navigation system (Brainsight version 2.2, Rogue Resolution Ltd., UK). High-resolution, T1-weighted anatomical scans of participants were obtained on a 3 T Magnetic Resonance Imaging (MRI) scanner (Siemens Skyra scanner, Siemens Healthcare, Germany) at HealthCare Global Hospital, Bangalore. Images were acquired with an MPRAGE sequence (TR = 2300 ms, TE = 2.32 ms, Field of View = 240 mm, flip angle = 8°, 256 voxel matrix size, Parallel acquisition technique (PAT) with in-plane acceleration factor 2, 32 channel head coil, voxel size 1 x 1 x 1 mm<sup>3</sup>). For 4/28 participants in the rPPC cTBS cohort, MRI scans could not be obtained due to logistical challenges. For these participants, the distance between the right and left tragus, and the inion and nasion were measured, and the scan of the participant with the most similar head measurements was used for neuro-navigation. The right PPC subdivision corresponding to the caudal-most extent of the third functional subdivision of the intraparietal sulcus (AICHA atlas, BA 7<sup>27</sup>) was targeted (Talairach coordinates: [26.5, 34, -65.5], MNI coordinates: [26,36,-69]). MR images were mapped from the scanner space to the MNI space to create a three-dimensional, curvilinear representation of each participant's brain, upon which the rPPC coordinates were projected. This was followed by registering a set of anatomical landmarks for each participant so that the position and orientation of the coil could be adjusted manually to the target location on the participant's head, in real time. The coil was held in position through the stimulation session with the help of an articulated mechanical arm. For resting motor threshold (RMT) determination, the coil was positioned using the Brainsight software by visually identifying the "omega" shaped hand knob area near the central sulcus. Then, the coil was moved in 1 cm increments (anterior, posterior, left, and right along a virtual grid) until large, clear MEPs and/or visible hand twitches were observed<sup>90</sup>.

**Neurostimulation protocol.** TMS was delivered with a MagPro X100 stimulator (Magventure A/S, Denmark) and a static cooled, figure-of-eight magnetic coil (MCF B65, Magventure). The coil was held tangentially to the skull, with the handle pointing backward and laterally at a 45-degree angle away from the midline.

Resting motor threshold (RMT) was determined for each participant by delivering single, biphasic pulses to the right motor cortex and measuring Motor Evoked Potentials (MEPs) elicited from the FDI muscle of the left hand in resting state. Ag-AgCl surface electrodes were used in a belly tendon montage on the FDI muscle (Kendall foam electrodes/ 3 M foam electrodes, 3 M India Ltd.), and the ulnar bone was used for placing the reference/ground electrode. RMT was defined as the machine output (intensity) at which an MEP equal to or above 50  $\mu$ V (peak to peak voltage) was elicited, in five out of ten pulses. After finding the optimal cortical location for the FDI muscle or motor hotspot, pulse intensity was reduced from 55% of maximum stimulator output (MSO), in steps of 2%, until RMT was reached. 18/28 participants showed consistent MEPs. In 10 participants for whom consistent MEPs could not be obtained in the FDI muscle despite prolonged search for the motor hotspot, we employed a subjective measure – stimulation intensity at which the participant reported a twitching



sensation (without overt movement) between their thumb and forefinger in half of the delivered pulses – as the participant's RMT. The range of RMTs was comparable between the two sub-groups (MEP-based RMT: 38–55% of MSO,  $n = 18$ ; subjective report-based RMT: 42–55%,  $n = 10$ ). Moreover, we observed nearly identical results even if the latter group of 10 participants (with a subjective report based RMTs) was excluded from all subsequent analyses.

The cTBS paradigm followed the one proposed by Goldsworthy et al. (2012)<sup>28</sup>, which has been reported to yield superlative suppression of MEP amplitudes. Biphasic pulses were delivered at 80% of the participant's RMT<sup>28</sup> in continuous bursts, each burst comprising 3 pulses with 33.3 ms between them (30 Hz). The inter-burst interval was 167 ms (6 Hz), and the entire protocol was completed in ~33 s ( $n = 600$  total pulses). For sham cTBS sessions the same procedure was followed, except that the coil was held perpendicular to, rather than tangential to, the scalp to avoid magnetic flux from entering the head, while simulating coil proximity and auditory sensations as in the actual cTBS.

**Behavioral testing with rPPC cTBS.** The rPPC cTBS group were trained and tested over two days. On the first day, each participant performed a training session comprising 7–12 task blocks of 50 trials each until they were able to detect changes successfully (average  $d' > 1.0$ ). Participants who performed the task successfully were then invited to participate in the main stimulation experiment, which was conducted within at most two days after training. Visual feedback was provided in the first two blocks of the training session informing the participant regarding the location of change or no change, and if their response was correct or incorrect. No feedback was provided in subsequent training blocks and all testing blocks in the stimulation experiment. Training data were excluded from further analyses.

The rPPC stimulation experiment involved two task sessions, comprising 5 blocks of 50 trials each; thus, each participant performed a total of 500 trials throughout the entire experiment. After determining the resting motor threshold (RMT), actual (or sham) cTBS was delivered to the rPPC. Immediately afterward, participants performed a task session of five blocks, which typically required 30 min to complete. After a 40 min rest interval, sham (or actual) cTBS was delivered, followed immediately by another task session of five blocks. The order of sham and actual cTBS sessions was counterbalanced across participants (see also SI Results section on *Additional control analyses for training and session order effects*).

**Motor cortex cTBS.** First, we identified the motor hotspot for FDI muscle stimulation and recorded participants' resting motor thresholds (RMT) with the procedure outlined previously (subsection on *Neurostimulation protocol*); in this case, the motor hot-spot and RMT were reliably determined in all (7/7) participants. We then determined baseline excitability as the median of the MEP elicited by 15 single pulses delivered at 110% of RMT. Then, cTBS was administered at 80% RMT over the motor hot-spot. MEP amplitudes were monitored at 5 min following stimulation and subsequently every 10 min, up to 60 min post stimulation. The median amplitude at each time point was compared to that at baseline, with Wilcoxon signed rank tests, to quantify the extent of suppression (or facilitation).

### Experimental procedure: tACS experiments

**Neurostimulation protocol.** We applied transcranial electrical stimulation (tES) over the left or the right PPC using a Soterix 4 × 1 HD-tES system (Soterix Medical Inc, New York, NY). A Soterix Medical HD cap – with electrode positions based on the international 10-10 system – was placed on the participant's scalp using the Cz electrode location as a reference. For each participant, we identified the Cz electrode location based on the intersection of the two lines connecting the left and right preauricular points (anterior to the left and right tragus, respectively)

and theinion and nasion. Sintered Ag-AgCl ring electrodes mounted on customized HDI Electrode Holders (Soterix Medical Inc) were placed in a 4 × 1 montage centered at the P4 location<sup>45,91</sup> (Supplementary Fig. S2d, e). HD-Gel conductive gel (Soterix Medical Inc) was used to provide electrical contact between the scalp and the electrodes. Electrode impedance was monitored throughout the experiment to ensure optimal contact quality (threshold: 0.5 quality units<sup>91</sup>). The duration (20 min), peak-to-peak amplitude, and frequency of stimulation were manually selected in the tES device before the experiment. The onset of stimulation was manually controlled, and stimulation commenced immediately before the start of each task session.

During the tACS stimulation session (Fig. 1c, right flowchart), transcranial alternating current was delivered at 40 Hz with a peak-to-peak amplitude of 1.5 mA ( $n = 16$  participants) or 2 mA ( $n = 10$  participants) for 20 min, including a ramp-up and ramp-down interval of 30 s, each. During the sham stimulation session (Fig. 1c, right flowchart), the current was ramped up for 30 s and then immediately ramped down to zero for 30 s; no stimulation was provided subsequently. Sham stimulation was delivered using the Auto-Sham setting on the tACS controller. Such ramping of currents mimics the somatosensory effect induced by real tES, which is the strongest when the currents ramp up or down in amplitude<sup>32,56</sup>. A two-way ANOVA with stimulation condition (sham, stim) and stimulation amplitude (1.5 mA, 2.0 mA) revealed no statistically significant main effect of stimulation amplitude on any parameter (HR:  $F_{1,48} = 1.48$ ,  $p = 0.230$ ; FA:  $F_{1,48} = 0.39$ ,  $p = 0.535$ ;  $d'$ :  $F_{1,48} = 0.71$ ,  $p = 0.404$ ; c:  $F_{1,48} = 3.55$ ,  $p = 0.066$ ). There was also no statistically significant interaction of stimulation condition and stimulation amplitude on any of the parameters (HR:  $F_{1,48} = 0.04$ ,  $p = 0.849$ ; FA:  $F_{1,48} = 1.2$ ,  $p = 0.278$ ;  $d'$ :  $F_{1,48} = 0.02$ ,  $p = 0.894$ ; c:  $F_{1,48} = 0.5$ ,  $p = 0.482$ ). Therefore, we combined the data across these cohorts ( $n = 26$ ) for all reported 40 Hz tACS results.

**Behavioral testing with rPPC tACS.** Participants were trained on the behavioral task one day before the main experiment. Training details are identical to those described for the cTBS cohort.

The neurostimulation experiment was conducted in 3 sessions: “sham”, real (“stim”), and “post” stimulation sessions, always conducted in that order. During each session, participants performed 5 blocks of 50 trials each of the cued multialternative orientation change detection task (Fig. 1a), for a total of 750 trials. Each session lasted around 20 min, with a 5 min break between the sham and stim sessions, and a 30 min break (“washout”) period between the stim and post sessions. No stimulation was applied during the post session. The entire experiment session lasted approximately 2 hours.

**Counterbalancing.** The fixed order of the sham-stim-post sessions in our study is the same as that employed in previous, seminal tACS studies<sup>32,33,35</sup>, and is motivated by the observation that tACS effects can persist for tens of minutes to >1h even after cessation of stimulation<sup>33,34</sup>. Consequently, our sham session always preceded the stim session to avoid any persistent effects of prolonged tACS stimulation from carrying over into the sham baseline. In addition, 30 min after the stimulation, behavioral performance was assessed in the post-stimulation session to confirm that stimulation effects had washed out and that performance had returned to pre-stimulation baseline after the entire experiment. To address any concern that the absence of counterbalancing in tACS could lead to training-related or stimulation-unrelated effects on behavior, we tested  $n = 26$  participants in a control experiment, described next.

**Control experiment.** We tested  $n = 26$  participants in a control experiment to test for training effects and to test for the specificity of effects with respect to the tACS stimulation frequency employed in the main experiment. In this case, participants received 60 Hz (instead of 40 Hz) tACS for 20 min over the rPPC in the actual stimulation session

(Supplementary Fig. S7a); none of the participants overlapped between this control cohort and 40 Hz (main experimental) cohort. 3 of the participants also underwent a 60 Hz stimulation session over the left PPC on a different day, separated by at least one week from the rPPC session; the remaining 23 participants underwent only rPPC stimulation. All other experimental protocols for the control experiment were identical to the main experimental session (Fig. 1c right).

Our choice of control tACS frequency (60 Hz) was inspired by previous studies that showed strong frequency dependency of behavioral effects, even within the gamma band<sup>46,92</sup>. For example, a recent study applied tACS at 40, 60, and 80 Hz over the primary visual cortex during a covert spatial attention task and observed a decrease in discrimination threshold only during 60 Hz stimulation but not for 40 and 80 Hz<sup>46</sup>. Similarly, a strong enhancement in visuo-motor performance was reported following 80 Hz tACS but not 5, 20 and 60 Hz tACS over the motor cortex<sup>92</sup>. While we could have chosen control frequencies of stimulation in neighbouring frequency bands (e.g., alpha band (8–12 Hz), theta band (4–8 Hz), or beta band (>20 Hz)), such oscillations are already associated with specific cognitive or motor functions (e.g., distractor suppression<sup>93</sup>, working memory<sup>94</sup>, or movement initiation<sup>95</sup>, respectively). Stimulating at these control frequencies may have produced behavioral effects (e.g., changes in RT due to motor inhibition) unrelated to our question of interest. Selecting 60 Hz as a control frequency strengthens our claim for a frequency-specific effect of 40 Hz rPPC tACS on psychophysical parameters. Such a frequency-specific effect also has a plausible physiological basis, given recent evidence of sharp frequency tuning of cortical inhibitory neurons<sup>63</sup>.

### Behavioral task

Participants were seated comfortably in an isolated room, 60 cm in front of a contrast-calibrated display monitor (22-inch LG LCD), with their head supported on a chin rest. Stimuli were programmed with Psychtoolbox (version 3.0.11) and MATLAB R2014b (Natick, MA), and an RB-840 response box (Cedrus Inc.) was used to record participants' responses.

A predictively cued, 3-alternative, attention task (Posner cueing task<sup>8,51</sup>) was used to assess the effect of rPPC stimulation. Participants detected grating orientation changes at one of two locations with probabilistic (predictive) spatial cues. The task protocols for the cTBS and tACS cohorts were nearly identical. In the cTBS experiment, stimulation was applied offline, and then the participants performed the 2-ADC behavioral task sessions (sham/pre- and stim/post-cTBS). In the tACS experiment, however, both the sham and actual stimulation were applied online for 20 min, per standard protocols<sup>35</sup>, during which the participants performed the 2-ADC task. Therefore, the durations of various task epochs had to be adjusted (shortened) for the latter experiment to fit within the 20 min window of tACS stimulation (Fig. 1a–c). Here, we report the task as performed by the participants in both cohorts; minor differences between the cTBS and tACS task stimulus timings are noted, parenthetically, in the following description (see also Fig. 1a).

Each trial began with the appearance of a fixation cross at the centre of a grey screen (0.5° diameter). Following a short fixation period (cTBS: 200 ms, tACS: 200 ms), two Gabor gratings appeared at a distance of 3.5° from the fixation cross along the horizontal meridian, one in each visual hemifield (s.d. = 0.6°; grating spatial frequency, 1.5 cycles/degree, full contrast, mean luminance 10 cd/m<sup>2</sup>), whose orientations were independently and pseudorandomly sampled from a uniform random distribution (0 to 180°) across trials and locations. Shortly after (cTBS: 250 ms, tACS: 250 ms), a central attention cue (directed 0.35° positive contrast line segment) appeared above the fixation cross. The cue remained on screen for a variable, exponentially distributed interval (cTBS: 300–1100 ms, mean: 2000 ms; tACS: 300–1100 ms, mean: 2000 ms). Then, the gratings briefly disappeared

(cTBS: 200 ms; tACS: 200 ms), and reappeared. Following reappearance, either one of the Gabors had changed in orientation, or none had changed (cTBS: 500 ms; tACS: 200 ms). The participant indicated the location of “change” (left or right) or “no change”, by pressing one of three buttons on the response box with their dominant hand (cTBS: 1000 ms response window; tACS: 1000 ms for  $n = 8$  and 1500 ms for  $n = 18$  in the main experiment; 1500 ms for all control experiments).

We term trials in which a change in orientation occurred at one of the two locations as “change” trials (80% of all trials), and trials with no change in orientation, as “no change” or “catch” trials (20% of all trials). On 75% of change trials, a change in orientation occurred at the cued location (80% cue validity); on the remaining 25% of change trials, the change occurred at the uncued location (Fig. 1b). The cue was equally likely to point toward the left or the right hemifield, sampled in pseudorandom order. Participants were not explicitly informed about the probabilities of the different event types but were informed that changes were more probable at the cued location than at the uncued location and that no changes could also occur at either of the locations.

The change angle at which neurostimulation would induce the strongest effect on  $d'$  could not be ascertained a priori. Therefore, for each participant, we measured the entire psychophysical function across a range of change angles ( $\Delta\theta$ , Figs. 2a, 4a, and Supplementary Fig. S4). For the cTBS experiments, orientation change angles ( $\Delta\theta$ ) were sampled from five different values (5°, 10°, 15°, 20°, 25°) equally and pseudorandomly, both at the cued and uncued locations for all  $n = 28$  participants. For the tACS experiments, orientation changes were sampled from among 5 orientations (5°, 9°, 15°, 26°, 45°) for  $n = 16$  participants in the main cohort and from a slightly different set (5°, 15°, 45°, 65°, 90°) for the remaining  $n = 10$  participants in the main cohort as well as the  $n = 26$  participants in the control cohort.

**Eye-tracking.** Fixation was monitored with an infrared eye-tracker (Gazepoint GP3; 60 Hz sampling rate). On each trial, gaze positions along the azimuth and elevation were stored for subsequent offline analysis. Trials in which the eye position deviated by more than 1.5 degrees from the fixation cross in the azimuthal direction, in a time window from stimulus onset until response, were flagged for rejection. Blinks were detected with a custom MATLAB code. Trials in which the tracker lost the location of the pupil for more than 100 ms continuously were also flagged for rejection. Upon applying these rejection criteria, median rejection rates were 7.2% ( $\pm 8.1$ %, std. dev) for the cTBS cohort and 5.6% ( $\pm 1.5$ %, std. dev) for the 40 Hz tACS cohort.

We tested whether excluding these trials would significantly alter the distribution of response proportions in the stimulus-response contingency table, using a randomization test based on the chi-squared statistic<sup>8</sup>. We found that contingency tables were statistically indistinguishable (Supplementary Fig. S1e, f) (median:  $p = 0.99$ ) before and after eye tracking-based rejection. Given the nearly indistinguishable distribution of response proportions, with or without eye-tracking rejection, all experimental trials were included in the analyses reported in the main text to avoid any systematic differences in task or stimulus parameters in these excluded trials from confounding the results when quantifying the effects of stimulation.

In addition, we performed a two-way ANOVA to compare the effects of stimulation condition (sham, stim) and trial type (cued change vs uncued change vs no change) on the rejection rates in each cohort. The analysis revealed no main effect of stimulation condition (cTBS:  $F_{1,54} = 1.16$ ,  $p = 0.291$ ; tACS:  $F_{1,50} = 1.59$ ,  $p = 0.214$ ) nor a significant interaction effect of stimulation condition and trial type on trial rejection rates (cTBS:  $F_{1,54} = 0.58$ ,  $p = 0.565$ ; tACS:  $F_{1,50} = 1.56$ ,  $p = 0.220$ ). In other words, the fixation performance was not statistically significantly different across trial types before and following stimulation.

### Analysis of psychometric parameters: Hit rates, false alarm rates, and reaction times

We analysed the effects of rPPC cTBS and tACS on behavioral accuracies and reaction times. Because our task was a cued, 3-alternative change detection task, each participant's behavioral responses were organized into a  $3 \times 3$  stimulus-response contingency table. Change locations and response locations in the left and right hemifields were represented in the first two rows and the first two columns, respectively. No-change events and responses were represented in the last row and last column, respectively. The contingency table was then transformed so that change events and responses were quantified relative to the cued location, pooling data across both hemifields. Following this transformation, the first two rows (first two columns) now represented change events (responses) at the cued and the uncued locations, respectively (Supplementary Fig. S1a).

The contingency table contains five categories of responses: hits (correct localization during change trials), misses (no change responses during change trials), false-alarms (change responses during no change trials), mislocalizations (incorrect localization during change trial), and correct rejections (no change responses during no-change trials). The proportion of each type of response was computed by dividing the number of responses in each cell by the total number of events in each row. We note that the proportion of misses and the proportion of correct rejections are not independent of the other response proportions (e.g., proportion of misses =  $1 - [\text{proportion of hits} + \text{proportion of mislocalizations}]$ ). Individual psychometric functions (performance as a function of orientation change angle) were computed and fit with a 3-parameter sigmoid function to hit rates across all change angle values at each location.

**Reaction times.** Reaction times were computed as the time from the change onset to the time of response (button press). Participants were instructed to respond as quickly as possible following the onset of the change stimulus (Fig. 1a). Responses that exceeded the maximum response time window (see Methods section on *Behavioral Task*) were not recorded. For each participant, RT values falling outside three standard deviations from the mean were marked as outliers and excluded from further analysis. Reaction times reported in the results (Supplementary Fig. S3a, b) correspond to averages at each location for correct change detection (hit) trials alone.

### Estimating psychophysical parameters: Sensitivity and Criterion

We examined the effect of rPPC cTBS on sensitivity and bias with a recent, multidimensional signal detection model – the m-ADC model – that was developed, specifically, for the analysis of attention tasks<sup>25,26</sup>. An elaborate description of the model is available from previous studies (e.g. Sridharan et al., 2017<sup>25</sup>; Banerjee et al., 2019<sup>5,25,26</sup>). Here, we provide a brief description and intuition of the model in two dimensions (2-ADC). Briefly, the participant's decision is modeled in a two-dimensional decision space based on a bivariate Gaussian decision variable  $\psi$ , which encodes the sensory evidence for a change at two stimulus locations (here, cued and uncued). Signal distributions – indicating evidence of change at each location – are represented along orthogonal axes (Supplementary Fig. S1b). The noise distribution, i.e., when no change in orientation occurs at either location, is centered at the origin. The mean of a signal distribution along each axis represents the average evidence for change and quantifies sensitivity ( $d'$ ) at the respective location. The participant employs different, independent decision thresholds ( $t_{\text{cued}}$  and  $t_{\text{uncued}}$ ) for each location. On each trial, the participant's decision is modeled as follows: the participant chooses to report change at whichever location the decision variable exceeds the decision threshold. If decision variables at both locations exceed their respective thresholds, the location at which the decision variable component exceeds its threshold by a greater magnitude is chosen for a change report. If the decision variable at neither location exceeds its

(respective) threshold, the participant indicates a “no change” response. As in conventional signal detection theory, the participant's criterion at each location is quantified based on the distance of the decision threshold at that location from the location of equal likelihood for signal and noise (intersection of the signal and noise distributions along the respective axis). The m-ADC model was fit to each participant's responses in the contingency table for sham and stimulation (and post) sessions independently for both cTBS and tACS cohorts. Goodness of fit  $p$ -values, with a randomization test based on the chi-squared statistic, for each cohort are reported in Supplementary Fig. S1c, d.

Sensitivity ( $d'$ ) and threshold ( $t$ ) were estimated at each location using a maximum likelihood estimation approach<sup>5,25</sup>. At each location (cued, uncued),  $d'$  was estimated for each change angle tested. At each location, a single, uniform decision threshold ( $t$ ) was estimated across all change angles; because of the pseudorandom distribution of change angles, it is reasonable to expect that participants could not anticipate the specific change angle on each trial and adjust their threshold accordingly. On the whole, a total of 12 parameters (10  $d'$  and 2 thresholds ( $t$ ); i.e., 5  $d'$  and one  $t$  for each of the two locations) were estimated. The criterion ( $c$ ) at each location (cued, uncued) was then estimated with the formula:  $c = t - d'_{\text{av}}/2$ , where  $d'_{\text{av}}$  refers to the average value of  $d'$  across all angles tested at that location<sup>8</sup>. The criterion is inversely related to the bias, such that the lower the criterion at a location, the higher the bias for reporting changes at that location<sup>96</sup>. Average  $d'$  values and the criteria are plotted in Figs. 3a–d, 5a–d for each participant and stimulation condition.

We computed the cue-induced change in sensitivity and bias as the difference between the value of the respective parameter ( $d'$ ,  $c$ ) between the cued and uncued locations ( $\Delta d' = d'_{\text{cued}} - d'_{\text{uncued}}$ ;  $\Delta c = c_{\text{cued}} - c_{\text{uncued}}$ ); we refer to this difference as the “attentional modulation” of  $d'$  or  $c$  in the text. Because an ANOVA did not reveal a significant interaction between change angle and stimulation condition (see Results), we reported the stimulation effect on  $\Delta d'$  averaged across angles tested. We also quantified the stimulation induced change in sensitivity or bias between the sham and stimulation sessions ( $\delta d' = d'_{\text{stim}} - d'_{\text{sham}}$ ;  $\delta c = c_{\text{stim}} - c_{\text{sham}}$ ) for each location (cued, uncued); this difference was also quantified for the attentional modulation (referred to as  $\delta_{\Delta}$ ).

### Statistical tests and model comparison analysis

**Statistical tests.** Pairwise comparisons of parameter values (HR, FAR,  $d'$ ,  $c$  and RT) between sham and stimulation (or sham and post) sessions, or their attentional modulations (e.g., Figs. 3c, d and 5c, d) were performed with non-parametric two-sided Wilcoxon signed rank tests;  $p$ -values were computed using normal approximation ( $z$ -statistic) due to sample size  $>15$  in all cohorts. Unless otherwise stated, we employed a Benjamini-Hochberg (BH) correction for multiple comparisons<sup>97</sup>;  $p$ -values were considered significant only if they passed a BH false discovery rate (FDR) threshold of 0.05. Absolute values of the effect sizes (Cohen's  $d$ ) were also computed for the pairwise comparisons, using a correction factor of  $\sqrt{1-r}$ , where  $r$  is the Pearson's correlation between the pairwise observations<sup>98</sup>. In addition, we compute and report 95% confidence intervals, condition-wise, for the change in parameter values induced by stimulation ( $\delta$ ). A two-way ANOVA was used to examine the effects of cueing (cued, uncued) and stimulation condition (sham, stim) on the attentional parameters. Unless otherwise stated, we performed a Shapiro-Wilk test of normality for the data before performing an ANOVA. In all cases, we found no evidence for deviation from normality (at the  $p = 0.05$  level); a Lilliefors' goodness-of-fit test for normality yielded essentially identical results. To test the laterality effects of the stimulation protocols, a two-way ANOVA was performed using stimulation condition (sham, stim) and change hemifield (ipsilateral change, contralateral change) for the parameters at the cued and uncued locations separately. We also tested if the strength of sensitivity and bias effects at the uncued location were



different between the two modalities of stimulation by performing a two-way ANOVA with stimulation type (cTBS, tACS) and stimulation condition (sham, stim).

Bayes factors were computed with the JASP software<sup>31</sup> and always reported as the ratio of the likelihood of the alternative hypothesis to the likelihood of the null hypothesis (e.g.,  $BF_{10}$ )<sup>99</sup>. We hypothesized that rPPC stimulation would produce a significant reorienting deficit in bias (increase in criterion) at the uncued location, and a corresponding increase in criterion modulation. Therefore, we computed a one-tailed Bayes factor to quantify evidence for an increase in the magnitude of criterion modulation (more negative  $\Delta c$ ;  $BF_{+0}$ ) or an increase in uncued criterion ( $BF_{-0}$ ) following cTBS or 40 Hz tACS stimulation using JZW priors<sup>100</sup>. We did not have an a priori hypothesis regarding the directionality of change in sensitivity ( $d'$ ) following rPPC stimulation. In this case, we computed a two-tailed Bayes factor ( $BF_{10}$ ) to quantify evidence for a change in sensitivity modulation, regardless of direction of change. In each case, the null hypothesis was an absence of change in modulation in the respective parameter ( $d'$  or  $c$ ) following stimulation. To compare parameter modulations between the sham and post sessions, as well as to compare the effects between the main (40 Hz) tACS and control (60 Hz) tACS experiments, we computed two-tailed Bayes factors ( $BF_{10}$ ), as we were agnostic to the direction of the effects. In addition, Bayesian sequential analysis robustness check was also performed with the JASP software.

To assess the goodness-of-fit of the m-ADC model to the behavioral data, we employed randomization tests based on the chi-squared statistic; the procedure is described in detail elsewhere<sup>5,25</sup>. To examine the effects of the order of rPPC tACS (before or after IPPC tACS), we performed a two-way ANOVA with stimulation condition (sham, stim) and stimulation session order (IPPC first, rPPC first). Similarly, another two-way ANOVA tested the effects of stimulation condition (sham, stim) and stimulation order (sham first, stim first) in the cTBS cohort.

**Model comparison analysis.** We performed a formal model comparison analysis to test whether rPPC stimulation effects could be better explained by either sensitivity changes or bias changes alone. We modified the m-ADC model with different constraints on  $d'$  and  $c$  to fit the behavioral effects of stimulation. In the first model – the “selective bias-effect” model – sensitivity values at each location during the actual stimulation session were constrained to be equal to their corresponding values during the sham session; this constraint served to model the scenario of no sensitivity change with neurostimulation. As a result, the sham session was fit with 12 parameters (10 for  $d'$  and 2 for  $t$ ), whereas the stimulation session was fit with 2 parameters (for  $t$  alone); values of  $d'$  were taken to be identical with their sham session values. In the second model – the “selective sensitivity-effect” model – threshold (criterion) values at each location during the actual stimulation session were constrained to be equal to their corresponding values during the sham session; this constraint served to model the scenario of no threshold (criterion) change with neurostimulation. In this case, the sham session was fit, as before, with 12 parameters (10 for  $d'$  and 2 for  $t$ ), whereas the stimulation session was fit with 10 parameters (for  $d'$  alone); values of  $t$  were taken to be identical with their sham session values. These more parsimonious models were compared with the standard m-ADC model that incorporated both sensitivity and criterion changes (“both-effects” model). The resultant three models were compared with the Bayesian Information Criterion (BIC; Figs. 3f, 5f) and the corrected Akaike Information Criterion (AICc; Supplementary Fig. S3c, d); computed as follows:

$$BIC = -2 \ln(L) + k \ln(n)$$

$$AICc = 2k - 2 \ln(L) + ((2k^2 + 2k)/(n - k - 1))$$

where  $k$  is the number of model parameters,  $n$  is the number of samples,  $L$  is the likelihood value based on the maximum likelihood model fit, and  $\ln()$  represents the natural logarithm function. Each information criterion quantifies a trade-off between model complexity and goodness-of-fit: a lower BIC or AICc score represents a better candidate model. BIC (and AICc) values were compared across all 3 models with Wilcoxon signed rank tests (Figs. 3f, 5f, Supplementary Fig. S3c, d)<sup>101</sup>.

### Reporting summary

Further information on research design is available in the Nature Portfolio Reporting Summary linked to this article.

### Data availability

The data generated and analyzed in this study have been deposited in an online database under the accession code: <https://doi.org/10.6084/m9.figshare.25125470>.

### Code availability

Analyses were performed with MATLAB (MathWorks, Natick, MA) and JASP. All codes used to generate the results and figures presented in this study are available in an online database at: <https://doi.org/10.6084/m9.figshare.25125470>.

### References

1. Corbetta, M. & Shulman, G. L. Control of goal-directed and stimulus-driven attention in the brain. *Nat. Rev. Neurosci.* **3**, 201–215 (2002).
2. Carrasco, M. Visual attention: The past 25 years. *Vis. Res.* **51**, 1484–1525 (2011).
3. Rahnev, D. et al. Attention induces conservative subjective biases in visual perception. *Nat. Neurosci.* **14**, 1513–1515 (2011).
4. Luo, T. Z. & Maunsell, J. H. R. Neuronal Modulations in Visual Cortex Are Associated with Only One of Multiple Components of Attention. *Neuron* **86**, 1182–1188 (2015).
5. Banerjee, S., Grover, S., Ganesh, S. & Sridharan, D. Sensory and decisional components of endogenous attention are dissociable. *J. Neurophysiol.* **122**, 1538–1554 (2019).
6. Sreenivasan, V. & Sridharan, D. Subcortical connectivity correlates selectively with attention’s effects on spatial choice bias. *Proc. Natl. Acad. Sci.* **116**, 19711–19716 (2019).
7. Kincade, J. M., Abrams, R. A., Astafiev, S. V., Shulman, G. L. & Corbetta, M. An Event-Related Functional Magnetic Resonance Imaging Study of Voluntary and Stimulus-Driven Orienting of Attention. *J. Neurosci.* **25**, 4593–4604 (2005).
8. Mesulam, M. M. Spatial attention and neglect: Parietal, frontal and cingulate contributions to the mental representation and attentional targeting of salient extrapersonal events. *Philos. Trans. R. Soc. B Biol. Sci.* **354**, 1325–1346 (1999).
9. Culham, J. C. & Kanwisher, N. G. Neuroimaging of cognitive functions in human parietal cortex. *Curr. Opin. Neurobiol.* **11**, 157–163 (2001).
10. Freedman, D. J. & Ibois, G. An Integrative Framework for Sensory, Motor, and Cognitive Functions of the Posterior Parietal Cortex. *Neuron* **97**, 1219–1234 (2018).
11. Bisley, J. W. & Goldberg, M. E. Attention, intention, and priority in the parietal lobe. *Annu. Rev. Neurosci.* **33**, 1–21 (2010).
12. Bressler, S. L., Tang, W., Sylvester, C. M., Shulman, G. L. & Corbetta, M. Top-Down Control of Human Visual Cortex by Frontal and Parietal Cortex in Anticipatory Visual Spatial Attention. *J. Neurosci.* **28**, 10056–10061 (2008).
13. Duecker, F. & Sack, A. T. The hybrid model of attentional control: New insights into hemispheric asymmetries inferred from TMS research. *Neuropsychologia* **74**, 21–29 (2015).



14. Hilgetag, C. C., Théoret, H. & Pascual-Leone, A. Enhanced visual spatial attention ipsilateral to rTMS-induced 'virtual lesions' of human parietal cortex. *Nat. Neurosci.* **4**, 953–957 (2001).
15. Molenberghs, P., Vandenberghe, R. R. C., Mesulam, M. M. & Peeters, R. Remapping Attentional Priorities: Differential Contribution of Superior Parietal Lobule and Intraparietal Sulcus. *Cereb. Cortex* **17**, 2703–2712 (2007).
16. Vandenberghe, R. & Gillebert, C. R. Parcellation of parietal cortex: Convergence between lesion-symptom mapping and mapping of the intact functioning brain. *Behav. Brain Res.* **199**, 171–182 (2009).
17. Corbetta, M., Patel, G. & Shulman, G. L. *The Reorienting System of the Human Brain: From Environment to Theory of Mind.* (2008).
18. Shulman, G. L. et al. Interaction of Stimulus-driven reorienting and expectation in ventral and dorsal frontoparietal and basal Ganglia-cortical networks. *J. Neurosci.* **29**, 4392–4407 (2009).
19. Posner, M. I. Orienting of attention. *Q. J. Exp. Psychol.* **32**, 3–25 (1980).
20. Mengotti, P., Käsbauer, A. S., Fink, G. R. & Vossel, S. Lateralization, functional specialization, and dysfunction of attentional networks. *Cortex* **132**, 206–222 (2020).
21. Ptak, R. & Schnider, A. The attention network of the human brain: Relating structural damage associated with spatial neglect to functional imaging correlates of spatial attention. *Neuropsychologia* **49**, 3063–3070 (2011).
22. Huang, Y. Z., Edwards, M. J., Rounis, E., Bhatia, K. P. & Rothwell, J. C. Theta burst stimulation of the human motor cortex. *Neuron* **45**, 201–206 (2005).
23. Giustiniani, A. et al. Effects of low-gamma tACS on primary motor cortex in implicit motor learning. *Behav. Brain Res.* **376**, 112170 (2019).
24. Benussi, A. et al. Exposure to gamma tACS in Alzheimer's disease: A randomized, double-blind, sham-controlled, crossover, pilot study. *Brain Stimul.* **14**, 531–540 (2021).
25. Sridharan, D., Steinmetz, N. A., Moore, T. & Knudsen, E. I. Distinguishing bias from sensitivity effects in multialternative detection tasks. *J. Vis.* **14**, 16 (2014).
26. Sridharan, D., Steinmetz, N. A., Moore, T. & Knudsen, E. I. Does the superior colliculus control perceptual sensitivity or choice bias during attention? Evidence from a multialternative decision framework. *J. Neurosci.* **37**, 480–511 (2017).
27. Joliot, M. et al. AICHA: An atlas of intrinsic connectivity of homotopic areas. *J. Neurosci. Methods* **254**, 46–59 (2015).
28. Goldsworthy, M. R., Pitcher, J. B. & Ridding, M. C. A comparison of two different continuous theta burst stimulation paradigms applied to the human primary motor cortex. *Clin. Neurophysiol.* **123**, 2256–2263 (2012).
29. Hubl, D. et al. Time course of blood oxygenation level-dependent signal response after theta burst transcranial magnetic stimulation of the frontal eye field. *Neuroscience* **151**, 921–928 (2008).
30. Sagar, V., Sengupta, R. & Sridharan, D. Dissociable sensitivity and bias mechanisms mediate behavioral effects of exogenous attention. *Sci. Rep.* **9**, 1–13 (2019).
31. Love, J. et al. JASP: Graphical statistical software for common statistical designs. *J. Stat. Softw.* **88**, 1–17 (2019).
32. Helfrich, R. F. et al. Entrainment of brain oscillations by transcranial alternating current stimulation. *Curr. Biol.* **24**, 333–339 (2014).
33. Neuling, T., Rach, S. & Herrmann, C. Orchestrating neuronal networks: sustained after-effects of transcranial alternating current stimulation depend upon brain states. *Front. Hum. Neurosci.* **7**, 161 (2013).
34. Kasten, F. H., Dowsett, J. & Herrmann, C. S. Sustained aftereffect of  $\alpha$ -tACS lasts up to 70 min after stimulation. *Front. Hum. Neurosci.* **10**, 245 (2016).
35. Helfrich, R. F. et al. Selective Modulation of Interhemispheric Functional Connectivity by HD-tACS Shapes Perception. *PLoS Biol.* **12**, e1002031 (2014).
36. Shadlen, M. N. & Newsome, W. T. Neural basis of a perceptual decision in the parietal cortex (Area LIP) of the rhesus monkey. *J. Neurophysiol.* **86**, 1916–1936 (2001).
37. Cohen, M. R. & Maunsell, J. H. R. Attention improves performance primarily by reducing interneuronal correlations. *Nat. Neurosci.* **12**, 1594–1600 (2009).
38. Steinmetz, N. A. & Moore, T. Eye Movement Preparation Modulates Neuronal Responses in Area V4 When Dissociated from Attentional Demands. *Neuron* **83**, 496–506 (2014).
39. Wyart, V., Nobre, A. C. & Summerfield, C. Dissociable prior influences of signal probability and relevance on visual contrast sensitivity. *Proc. Natl. Acad. Sci. USA* **109**, 3593–3598 (2012).
40. Tarasi, L., di Pellegrino, G. & Romei, V. Are you an empiricist or a believer? Neural signatures of predictive strategies in humans. *Prog. Neurobiol.* **219**, 102367 (2022).
41. Lovejoy, L. P. & Krauzlis, R. J. Changes in perceptual sensitivity related to spatial cues depends on subcortical activity. *Proc. Natl. Acad. Sci. Usa.* **114**, 6122–6126 (2017).
42. Chinchani, A. M. et al. Tracking momentary fluctuations in human attention with a cognitive brain-machine interface. *Commun. Biol.* **5**, 1–17 (2022).
43. Opitz, A., Windhoff, M., Heidemann, R. M., Turner, R. & Thielscher, A. How the brain tissue shapes the electric field induced by transcranial magnetic stimulation. *Neuroimage* **58**, 849–859 (2011).
44. Thielscher, A., Opitz, A. & Windhoff, M. Impact of the gyral geometry on the electric field induced by transcranial magnetic stimulation. *Neuroimage* **54**, 234–243 (2011).
45. Datta, A. et al. Gyri-precise head model of transcranial direct current stimulation: Improved spatial focality using a ring electrode versus conventional rectangular pad. *Brain Stimul.* **2**, 201–207 (2009).
46. Laczó, B., Antal, A., Niebergall, R., Treue, S. & Paulus, W. Transcranial alternating stimulation in a high gamma frequency range applied over V1 improves contrast perception but does not modulate spatial attention. *Brain Stimul.* **5**, 484–491 (2012).
47. Di Lazzaro, V. et al. Theta-burst repetitive transcranial magnetic stimulation suppresses specific excitatory circuits in the human motor cortex. *J. Physiol.* **565**, 945–950 (2005).
48. Huang, Y. Z., Chen, R. S., Rothwell, J. C. & Wen, H. Y. The after-effect of human theta burst stimulation is NMDA receptor dependent. *Clin. Neurophysiol.* **118**, 1028–1032 (2007).
49. Rahnev, D. et al. Continuous theta burst transcranial magnetic stimulation reduces resting state connectivity between visual areas. *J. Neurophysiol.* **110**, 1811–1821 (2013).
50. Antal, A. & Paulus, W. Transcranial alternating current stimulation (tACS). *Front. Hum. Neurosci.* **7**, 317 (2013).
51. Krause, M. R., Vieira, P. G., Csorba, B. A., Pilly, P. K. & Pack, C. C. Transcranial alternating current stimulation entrains single-neuron activity in the primate brain. *Proc. Natl. Acad. Sci. Usa.* **116**, 5747–5755 (2019).
52. Zaehle, T., Rach, S. & Herrmann, C. S. Transcranial Alternating Current Stimulation Enhances Individual Alpha Activity in Human EEG. *PLoS One* **5**, e13766 (2010).
53. Vossen, A., Gross, J. & Thut, G. Alpha power increase after transcranial alternating current stimulation at alpha frequency ( $\alpha$ -tACS) reflects plastic changes rather than entrainment. *Brain Stimul.* **8**, 499–508 (2015).
54. Guerra, A. et al. Boosting the LTP-like plasticity effect of intermittent theta-burst stimulation using gamma transcranial alternating current stimulation. *Brain Stimul.* **11**, 734–742 (2018).

55. Moliadze, V., Atalay, D., Antal, A. & Paulus, W. Close to threshold transcranial electrical stimulation preferentially activates inhibitory networks before switching to excitation with higher intensities. *Brain Stimul.* **5**, 505–511 (2012).
56. Hopfinger, J. B., Parsons, J. & Fröhlich, F. Differential effects of 10-Hz and 40-Hz transcranial alternating current stimulation (tACS) on endogenous versus exogenous attention. *Cogn. Neurosci.* **8**, 102–111 (2017).
57. Hoy, K. E. et al. The effect of  $\gamma$ -tACS on working memory performance in healthy controls. *Brain Cogn.* **101**, 51–56 (2015).
58. Pahor, A. & Jaušovec, N. The effects of theta and gamma tacs on working memory and electrophysiology. *Front. Hum. Neurosci.* **11**, 651 (2018).
59. Nowak, M. et al. Driving human motor cortical oscillations leads to behaviorally relevant changes in local GABAA inhibition: A tACS-TMS study. *J. Neurosci.* **37**, 4481–4492 (2017).
60. Rufener, K. S., Zaehle, T., Oechslin, M. S. & Meyer, M. 40 Hz-Transcranial alternating current stimulation (tACS) selectively modulates speech perception. *Int. J. Psychophysiol.* **101**, 18–24 (2016).
61. Kasten, F. H., Wendeln, T., Stecher, H. I. & Herrmann, C. S. Hemisphere-specific, differential effects of lateralized, occipital–parietal  $\alpha$ - versus  $\gamma$ -tACS on endogenous but not exogenous visual-spatial attention. *Sci. Rep.* **10**, 1–11 (2020).
62. Van Kerkoerle, T. et al. Alpha and gamma oscillations characterize feedback and feedforward processing in monkey visual cortex. *Proc. Natl. Acad. Sci. USA.* **111**, 14332–14341 (2014).
63. Cardin, J. A. et al. Driving fast-spiking cells induces gamma rhythm and controls sensory responses. *Nature* **459**, 663–667 (2009).
64. Iaccarino, H. F. et al. Gamma frequency entrainment attenuates amyloid load and modifies microglia. *Nature* **540**, 230–235 (2016).
65. Zhou, D. et al. Effects of 40 Hz transcranial alternating current stimulation (tACS) on cognitive functions of patients with Alzheimer’s disease: a randomised, double-blind, sham-controlled clinical trial. *J. Neurol. Neurosurg. amp; Psychiatry* **93**, 568 LP–568 70 (2022).
66. Indovina, I. & Macaluso, E. Occipital-parietal interactions during shifts of exogenous visuospatial attention: Trial-dependent changes of effective connectivity. *Magn. Reson. Imaging* **22**, 1477–1486 (Elsevier Inc., 2004).
67. Gillebert, C. R. et al. Lesion evidence for the critical role of the intraparietal sulcus in spatial attention. *Brain* **134**, 1694–1709 (2011).
68. Roy, L. B., Sparing, R., Fink, G. R. & Hesse, M. D. Modulation of attention functions by anodal tDCS on right PPC. *Neuropsychologia* **74**, 96–107 (2015).
69. Porciello, G., Crostella, F., Liuzza, M. T., Valentini, E. & Aglioti, S. M. rTMS-induced virtual lesion of the posterior parietal cortex (PPC) alters the control of reflexive shifts of social attention triggered by pointing hands. *Neuropsychologia* **59**, 148–156 (2014).
70. Kalla, R., Muggleton, N. G., Juan, C.-H. H., Cowey, A. & Walsh, V. The timing of the involvement of the frontal eye fields and posterior parietal cortex in visual search. *Neuroreport* **19**, 1069–1073 (2008).
71. Vossel, S., Thiel, C. M. & Fink, G. R. Cue validity modulates the neural correlates of covert endogenous orienting of attention in parietal and frontal cortex. *Neuroimage* **32**, 1257–1264 (2006).
72. Ruff, C. C. et al. Distinct causal influences of parietal versus frontal areas on human visual cortex: Evidence from concurrent TMS-fMRI. *Cereb. Cortex* **18**, 817–827 (2008).
73. Bergmann, T. O., Karabanov, A., Hartwigsen, G., Thielscher, A. & Siebner, H. R. Combining non-invasive transcranial brain stimulation with neuroimaging and electrophysiology: Current approaches and future perspectives. *Neuroimage* **140**, 4–19 (2016).
74. Mesulam, M. A cortical network for directed attention and unilateral neglect. *Ann. Neurol.* **10**, 309–25 (1981).
75. Vuilleumier, P. & Landis, T. Illusory contours and spatial neglect. *Neuroreport* **9**, 2481–2484 (1998).
76. Vuilleumier, P. & Rafal, R. ‘Both’ means more than ‘two’: localizing and counting in patients with visuospatial neglect. *Nat. Neurosci.* **2**, 783–784 (1999).
77. Corbetta, M., Kincade, J. M., Ollinger, J. M., Mcavoy, M. P. & Shulman, G. L. Voluntary orienting is dissociated from target detection in human posterior parietal cortex. *Nat Neurosci* **3**, 292–297 (2000).
78. Capotosto, P. et al. Anatomical segregation of visual selection mechanisms in human parietal cortex. *J. Neurosci.* **33**, 6225–6229 (2013).
79. Vandenberghe, R. & Gillebert, C. R. Dissociations between spatial-attentional processes within parietal cortex: Insights from hybrid spatial cueing and change detection paradigms. *Front. Hum. Neurosci.* **7**, 1–11 (2013).
80. Kiani, R. & Shadlen, M. N. Representation of confidence associated with a decision by neurons in the parietal cortex. *Science* **324**, 759–764 (2009).
81. Hwang, E. J., Dahlen, J. E., Mukundan, M. & Komiyama, T. History-based action selection bias in posterior parietal cortex. *Nat. Commun.* **8**, 1–14 (2017).
82. Hanks, T. D., Ditterich, J. & Shadlen, M. N. Microstimulation of macaque area LIP affects decision-making in a motion discrimination task. *Nat. Neurosci.* **9**, 682–689 (2006).
83. Kay, K. N. & Yeatman, J. D. Bottom-up and top-down computations in word- and face-selective cortex. *Elife* **6**, 1–29 (2017).
84. Silvanto, J., Muggleton, N., Lavie, N. & Walsh, V. The perceptual and functional consequences of parietal top-down modulation on the visual cortex. *Cereb. Cortex* **19**, 327–330 (2009).
85. Iemi, L., Chaumon, M., Crouzet, S. M. & Busch, N. A. Spontaneous neural oscillations bias perception by modulating baseline excitability. *J. Neurosci.* **37**, 807–819 (2017).
86. Di Luzio, P., Tarasi, L., Silvanto, J., Avenanti, A. & Romei, V. Human perceptual and metacognitive decision-making rely on distinct brain networks. *PLoS Biol.* **20**, 1–19 (2022).
87. Katz, L. N., Yates, J. L., Pillow, J. W. & Huk, A. C. Dissociated functional significance of decision-related activity in the primate dorsal stream. *Nature* **535**, 285–288 (2016).
88. Zhou, Y. & Freedman, D. J. Posterior parietal cortex plays a causal role in perceptual and categorical decisions. *Science* **365**, 180–185 (2019).
89. Sengupta, A., Banerjee, S., Ganesh, S., Grover, S. & Sridharan, D. The right posterior parietal cortex mediates spatial reorienting of attentional choice bias. *figshare. Dataset.* (2024) <https://doi.org/10.6084/m9.figshare.25125470>.
90. Borojerd, B. et al. Localization of the motor hand area using transcranial magnetic stimulation and functional magnetic resonance imaging. *Clin. Neurophysiol.* **110**, 699–704 (1999).
91. Villamar, M. F. et al. Technique and considerations in the use of 4x1 ring high-definition transcranial direct current stimulation (HD-tDCS). *J. Vis. Exp.* 1–15 (2013) <https://doi.org/10.3791/50309>.
92. Santarnecchi, E. et al. High-gamma oscillations in the motor cortex during visuo-motor coordination: A tACS interferential study. *Brain Res. Bull.* **131**, 47–54 (2017).
93. Gutteling, T. P., Sillekens, L., Lavie, N. & Jensen, O. Alpha oscillations reflect suppression of distractors with increased perceptual load. *Prog. Neurobiol.* **214**, 102285 (2022).
94. Mizuhara, H. & Yamaguchi, Y. Human cortical circuits for central executive function emerge by theta phase synchronization. *Neuroimage* **36**, 232–244 (2007).

95. Zaghi, S. et al. Inhibition of motor cortex excitability with 15Hz transcranial alternating current stimulation (tACS). *Neurosci. Lett.* **479**, 211–214 (2010).
96. Green, D. M. & Swets, J. A. *Signal detection theory and psychophysics*. (John Wiley and Sons, 1966).
97. Thissen, D., Steinberg, L. & Kuang, D. Quick and Easy Implementation of the Benjamini-Hochberg Procedure for Controlling the False Positive Rate in Multiple Comparisons. *J. Educ. Behav. Stat.* **27**, 77–83 (2002).
98. Cohen, J. *Statistical Power Analysis for the Behavioral Sciences (Second Edition)*. *Analytical Biochemistry* vol. 11 (1988).
99. Schönbrodt, F. D. & Wagenmakers, E. J. Bayes factor design analysis: Planning for compelling evidence. *Psychon. Bull. Rev.* **25**, 128–142 (2018).
100. Rouder, J. N., Speckman, P. L., Sun, D., Morey, R. D. & Iverson, G. Bayesian t tests for accepting and rejecting the null hypothesis. *Psychon. Bull. Rev.* **16**, 225–237 (2009).
101. Vrieze, S. I. Model selection and psychological theory: A discussion of the differences between the Akaike information criterion (AIC) and the Bayesian information criterion (BIC). *Psychol. Methods* **17**, 228–243 (2012).

## Acknowledgements

We thank Sourav Mukherjee and Sandarsh Pandey for assistance with data collection. We thank Sricharan Sunder and Priyanka Gupta for their feedback on a preliminary version of this manuscript. This research was supported by a Department of Biotechnology-Wellcome Trust India Alliance Intermediate fellowship (IA/I/15/2/502089), a Department of Science and Technology Swarna Jayanti Fellowship (SB/SJF/2021-22/02), a Pratiksha Trust Intramural grant (KVCH/22/2047), a Gore Subraya Bhat Chair Associate Professorship in Digital Health and an India-Trento Program for Advanced Research grant (INT/ITALY/ITPAR-IV/COG/2018/G) (all to DS), and an Institute of Eminence (IoE) grant, funded by the University Grants Commission (to IISc).

## Author contributions

D.S. conceptualized the study and wrote the paper. A.S. performed the tACS experiments, analyzed data, and wrote the paper. S.B. performed the cTBS experiments, analyzed data, and wrote the paper. S.Gr. performed cTBS experiments. S.Ga. performed cTBS experiments and analyzed data.

## Competing interests

The authors declare no competing interests.

## Additional information

**Supplementary information** The online version contains supplementary material available at <https://doi.org/10.1038/s41467-024-51283-z>.

**Correspondence** and requests for materials should be addressed to Devarajan Sridharan.

**Peer review information** *Nature Communications* thanks Justin Riddle, and the other, anonymous, reviewers for their contribution to the peer review of this work.

**Reprints and permissions information** is available at <http://www.nature.com/reprints>

**Publisher's note** Springer Nature remains neutral with regard to jurisdictional claims in published maps and institutional affiliations.

**Open Access** This article is licensed under a Creative Commons Attribution-NonCommercial-NoDerivatives 4.0 International License, which permits any non-commercial use, sharing, distribution and reproduction in any medium or format, as long as you give appropriate credit to the original author(s) and the source, provide a link to the Creative Commons licence, and indicate if you modified the licensed material. You do not have permission under this licence to share adapted material derived from this article or parts of it. The images or other third party material in this article are included in the article's Creative Commons licence, unless indicated otherwise in a credit line to the material. If material is not included in the article's Creative Commons licence and your intended use is not permitted by statutory regulation or exceeds the permitted use, you will need to obtain permission directly from the copyright holder. To view a copy of this licence, visit <http://creativecommons.org/licenses/by-nc-nd/4.0/>.

© The Author(s) 2024